

NETWORK CODED MULTI-HOP WIRELESS COMMUNICATION NETWORKS: CHANNEL ESTIMATION AND TRAINING DESIGN

Mugen Peng, *Senior Member, IEEE*, Qiang Hu, Xinqian Xie, Zhongyuan Zhao, and H. Vincent Poor, *Fellow, IEEE*

Abstract—User cooperation based multi-hop wireless communication networks (MH-WCNs) as the key communication technological component of mobile social networks (MSNs) should be exploited to enhance the capability of accumulating data rates and extending coverage flexibly. As one of the most promising and efficient user cooperation techniques, network coding can increase the potential cooperation performance gains among selfishly driven users in MSNs. To take full advantages of network coding in MH-WCNs, a network coding transmission strategy and its corresponding channel estimation technique are studied in this paper. Particularly, a 4-hop network coding transmission strategy is presented first, followed by an extension strategy for the arbitrary $2N$ -hop scenario ($N \geq 2$). The linear minimum mean square error (LMMSE) and maximum-likelihood (ML) channel estimation methods are designed to improve the transmission quality in MH-WCNs. Closed form expressions in terms of the mean squared error (MSE) for the LMMSE channel estimation method are derived, which allows the design of the optimal training sequence. Unlike the LMMSE method, it is difficult to obtain closed-form MSE expressions for the nonlinear ML channel estimation method. In order to accomplish optimal training sequence design for the ML method, the Cramér-Rao lower bound (CRLB) is employed. Numerical results are provided to corroborate the proposed analysis, and the results demonstrate that the analysis is accurate and the proposed methods are effective.

Index Terms—Multi-hop wireless communication networks, mobile social networks, network coding, channel estimation, training design.

I. INTRODUCTION

With the dramatic evolution of mobile communication systems and the rapid rise in the use of advanced mobile devices, the original web-based social networks have comprehensively penetrated into the mobile platform in recent years, motivating the newly emerged research field of mobile

social networks (MSNs) [1]. Currently, a large proportion of global communication traffic is contributed by user-generated activities associated with MSNs, e.g., instant messages, document sharing, and interactions within friend circles. MSNs have been characterized as pervasive and omnipotent mobile communication platforms involving social relationships via which users can search, share and deliver data anytime and anywhere [2].

Since MSNs encourage new modes of socially driven information flow and provide a backbone for modern communications, they have motivated considerable research interest for more than a decade. Most earlier studies of MSNs concentrated on human interactions and relations. More recently, considerable work has been devoted to addressing the intersection and interplay of online social networks and wireless communications from a technological viewpoint [3] [4], and rapid development in wireless communications have essentially driven the expansion of MSNs [5].

Despite this research effort, there are few existing works addressing the interplay between technological networks and social networks in MSNs. Some promising attempts at exploiting this interplay have been reported in [6], including security and privacy problems [7], network design [8] and efficient resource management [9]. Even so, there are still many unexplored significant technological challenges in the development of MSNs, which could lead to optimal design for socially based technological networks to offer better user experiences and services.

Stimulated by socially driven incentives, users in MSNs are willing to interact with others via sharing or delivering information voluntarily, which is referred to as initiative user cooperation [10]. Thereby, cooperative communication, regarded as an effective way to accumulate data rates and extend coverage flexibly [11], can improve the performance of MSNs by taking advantages of socially enabled collaborative features. Due to physical constraints, information exchange between two socially linked users in MSNs may need the cooperation of intermediate users in the underlying technological network, resulting in multi-hop wireless communication networks (MH-WCNs). As one of the most promising and efficient user cooperation techniques, network coding [12] has significant potential to further improve the performance of MH-WCNs. The intense research effort on network coded MH-WCNs has established that significant performance gains can be obtained with network coding. Sengupta, *et al.* analyzed throughput

Manuscript received Apr. 17, 2013; revised Sep. 15, 2014; accepted Nov. 07, 2014. The work of M. Peng, Q. Hu, X. Xie, and Z. Zhao was supported in part by the National Natural Science Foundation of China (Grant No. 61222103), the National High Technology Research and Development Program of China (Grant No. 2014AA01A701), and the Chinese State Major Science and Technology Special Project (Grant No. 2013ZX03001001). The work of H. V. Poor was supported in part by the U.S. National Science Foundation under Grant ECCS-1343210.

M. Peng, Q. Hu, X. Xie, and Z. Zhao are with the Key Laboratory of Universal Wireless Communications, Ministry of Education, Beijing University of Posts & Telecommunications, Beijing, China. Mugen Peng is also with the School of Engineering and Applied Science, Princeton University, Princeton, NJ, USA (e-mail: pmg@bupt.edu.cn; xxnbupt@gmail.com; hq760001570@gmail.com; zyzhao@bupt.edu.cn).

H. V. Poor is with the School of Engineering and Applied Science, Princeton University, Princeton, NJ, USA (e-mail: poor@princeton.edu).

improvements obtained by network coding for MH-WCNs in [13]. Network coding can also be incorporated into communication protocols for enhancing the reliability and speed of data gathering in smart grids [14] and wireless sensor networks [15]. Opportunistic network coding for optimization of routing strategies was introduced for wireless mesh networks in [16]. Further, the feasibility of network coding for applications in MSNs and its capacity to facilitate user cooperation have been demonstrated in [17]. However, to the best of our knowledge, how to design efficient network coded transmission strategies and how to implement network coding in practical radio channels for MH-WCNs are still not straightforward, which are key challenges to promote the commercial development of MSNs.

Since network coding enables each node to use coding operations on several packets [18], the nodes in network coded MH-WCNs need to mitigate the redundant self-interference through acquiring the necessary channel state information (CSI). Therefore, suitable network coding strategies and corresponding channel estimation methods are indispensable for network coded MH-WCNs. In [19], Gao, *et al.* provided a preliminary study of training based channel estimation issues for network coded two-way relay networks (TWRNs). Further, channel estimation in TWRNs with power allocation at intermediate nodes was further investigated in [20]. Afterwards, maximum a posteriori probability (MAP) based channel estimation algorithm was developed for TWRNs in [21]. The authors in [22] have shown that performance of network coded TWRNs significantly degrades under imperfect CSI conditions. The existing works for channel estimation and training design in network coding are mainly concentrated on 2-hop TWRNs, where the network coding strategy is relatively simple as the data decoding and channel estimation are only required at the desired nodes. Moreover, the performance of traditional training designs is good enough for 2-hop TWRNs owing to no requirements of channel estimation at the intermediate node. However, the extensions of network coding strategy, training design, and channel estimation from 2-hop TWRNs to MH-WCNs are not straightforward. Actually, these extensions are challenging due to the fact that self-interference cancelation and acquisition of CSI in MH-WCNs are required at both intermediate and desired nodes. Further, the general network coding transmission strategy for the arbitrary hops in MH-WCNs is still a topic for research. Consequently, it is of interest to develop an effective network coding strategy, and its corresponding channel estimation and training design for MH-WCNs.

Driven by solving these aforementioned extensions, an adaptive network coded multi-hop strategy is presented in this paper to improve the transmission spectral efficiency of MH-WCNs, which results in enhancing the performance of MSNs. Further, channel estimation and corresponding training design schemes are proposed to improve the transmission quality of MH-WCNs and to support practical implementations of network coded MH-WCNs. The main contributions are listed as follows.

- A network coded multi-hop transmission strategy for MH-WCNs is proposed, which can enable the periodic

reception of data symbols at the desired nodes, and achieve twofold spectral efficiency performance gains compared with the traditional point-to-point strategy.

- To guarantee that each intermediate node obtains the required CSI accurately, a suitable training scheme is designed, where not only the desired nodes but also the selected intermediate nodes are allowed to transmit training sequences, which can reduce overall resource consumption needed for training.
- Focusing on the special 4-hop scenario, both the linear minimum mean square error (LMMSE) and maximum-likelihood (ML) channel estimation methods for composite channel coefficients at desired nodes are proposed. Furthermore, the optimal training sequences aiming at minimizing the LMMSE-based mean squared error (MSE) and the ML-based Cramér-Rao lower bound (CRLB) performance metrics are derived for LMMSE and ML methods, respectively. This network coded 4-hop transmission strategy and the corresponding channel estimation methods are extended to the arbitrary $2N$ -hop scenario ($N \geq 2$). Simulation results indicate the effectiveness of the proposed estimators in improving the estimation accuracy and achieving significant performance gains over the traditional point-to-point estimation scheme.

The rest of this paper is organized as follows. In Section II, the relationship between MSNs and MH-WCNs is explained, and the network coding strategy in 4-hop WCNs is presented. Section III describes the LMMSE and ML channel estimation methods for the composite channel coefficients. The training design techniques for the channel estimation methods are discussed in Section IV. In Section V, the network coding strategy and the corresponding training design schemes in a general $2N$ -hop WCNs are described. Simulation results are presented in Section V to verify the proposed network coded transmission strategy, and the corresponding channel estimation and training design schemes. Finally, we offer conclusions in Section VI, followed by the related proofs in the appendix.

Notation: Vectors and matrices are denoted by boldface small and capital letters, respectively. The transpose, complex conjugate, Hermitian, inverse, and pseudo-inverse of the matrix \mathbf{A} are denoted by \mathbf{A}^T , \mathbf{A}^* , \mathbf{A}^H , \mathbf{A}^{-1} and \mathbf{A}^\dagger , respectively. $\text{tr}(\mathbf{A})$ is the trace of \mathbf{A} , and $\text{diag}\{\mathbf{A}\}$ denotes a diagonal matrix constructed from diagonal elements of \mathbf{A} . $[\mathbf{A}]_{ij}$ represents the (i, j) -th element of \mathbf{A} and \mathbf{I} is the identity matrix. $\|\mathbf{a}\|$ denotes the 2-norm of the vector \mathbf{a} . $\Re\{\cdot\}$ and $\Im\{\cdot\}$ denote the real and the imaginary part of the complex argument; $\mathcal{E}\{\cdot\}$ denotes the statistical expectation.

II. SYSTEM MODEL FOR 4-HOP WCNs

An MSN consisting of both wireless and social contacts can be characterized as a two-layer heterogeneous network, which is depicted in Fig. 1. The communication networking layer (lower layer) represents the overall radio communication links amongst different users, while the upper one depicts the social communication links amongst users. The social

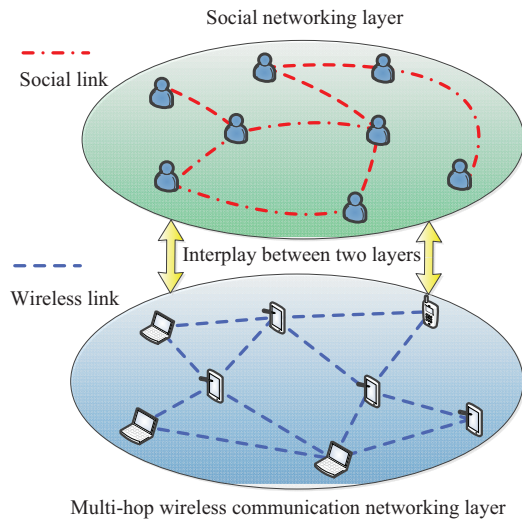


Fig. 1. System architecture for MSNs

layer is relational to the virtual communication as any two users can potentially form a contact link. On the contrary, the radio communication links are constrained by physical constraints, such as transmission distance, radio interference and transmission power, which results in possible difficulty in establishing a direct communication link between any two arbitrary users. Hence, link formation between two arbitrary users in the social layer of MSNs may transform into a multi-hop communication link with the help of user cooperation in the underlying communication networking layer. This fact indicates the strong interplay between these two layers and the emerging demand for the design of underlying multi-hop radio communication links to enable social communication in the upper layer.

To guarantee the quality and robustness of social links in MSNs, radio communication links should be connected adaptively. Denoting each user or each data source as a communication node, and regarding the wireless connection between adjacent users as a communication link, two arbitrary users can communicate with each other in a bidirectional manner. Thus, the multi-hop communication links in the underlying communication networking layer can be modeled as an MH-WCN from the technological viewpoint. To improve the spectral efficiency of MH-WCNs, network coding can be exploited. For the convenience of understanding, we firstly consider simple 4-hop MSNs as a paradigm in this paper, where two nodes are randomly selected to exchange information with each other via three intermediate communication nodes.

The system model for the network coded 4-hop WCNs, consisting of two communication nodes \mathbb{T}_1 and \mathbb{T}_2 and three cooperative communication nodes \mathbb{R}_1 , \mathbb{R}_2 and \mathbb{R}_3 , is shown in Fig. 2. Each node is equipped with a single antenna, and the half-duplex communication protocol is adopted in the intermediate nodes for information exchange. The transmission powers for nodes \mathbb{T}_1 , \mathbb{T}_2 , \mathbb{R}_1 , \mathbb{R}_2 , \mathbb{R}_3 are set to be P_1 , P_2 , P_{r1} , P_{r2} , P_{r3} , respectively. The data symbol sent by \mathbb{T}_i is denoted by x_i ($i = 1, 2$). The radio channel between any two adjacent

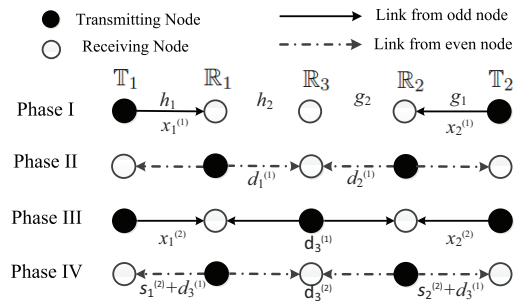


Fig. 2. Network coding transmission strategy for 4-hop WCNs.

communication nodes is assumed to be quasi-flat fading, and the channel response of the i -th hop from the communication node \mathbb{T}_1 to the intermediate node \mathbb{R}_3 is denoted by $h_i \in \mathcal{CN}(0, \sigma_{2i-1}^2)$ ($i = 1, 2$). Similarly, $g_i \in \mathcal{CN}(0, \sigma_{2i}^2)$ ($i = 1, 2$) denotes the channel coefficient of the i -th hop from \mathbb{T}_2 to \mathbb{R}_3 . Since this paper is focused on channel estimation and training design for MH-WCNs, the communication nodes are assumed to be synchronous, which can be fulfilled through synchronization technologies such as the global positioning system (GPS), post-facto synchronization [24], etc.

For traditional 4-hop WCNs, if \mathbb{T}_1 and \mathbb{T}_2 want to exchange information with each other, each desired node occupies 4 time phases to deliver its information to the destination node, and there are a total of 8 phases to fulfill this information exchange. To improve the spectral efficiency, the network coding transmission strategy is proposed in this paper, which can complete the information exchange in 4 phases. In the first phase, the desired nodes \mathbb{T}_1 and \mathbb{T}_2 transmit their information $x_1^{(1)}$ and $x_2^{(1)}$ simultaneously to \mathbb{R}_1 and \mathbb{R}_2 , respectively. \mathbb{R}_1 and \mathbb{R}_2 amplify their received signals and broadcast them to neighboring nodes in the second phase. In the third phase, \mathbb{T}_1 and \mathbb{T}_2 transmit new information $x_1^{(2)}$ and $x_2^{(2)}$ simultaneously to \mathbb{R}_1 and \mathbb{R}_2 , respectively, and \mathbb{R}_3 broadcasts the compound signal of $x_1^{(1)}$ and $x_2^{(1)}$ to both \mathbb{R}_1 and \mathbb{R}_2 . Both \mathbb{R}_1 and \mathbb{R}_2 broadcast the received compound signal and new information (i.e., $x_1^{(2)}$ and $x_2^{(2)}$) to adjacent nodes in the fourth phase. Based on the received information, \mathbb{T}_1 and \mathbb{T}_2 can exchange their information with each other, and \mathbb{R}_3 can obtain the compound signal of $x_1^{(2)}$ and $x_2^{(2)}$.

A. Network Coding Transmission Strategy in 4-Hop WCNs

As noted above, to accomplish the information exchange between the desired nodes \mathbb{T}_1 and \mathbb{T}_2 , data transmission for the network coded 4-hop WCNs is divided into 4 phases. In the first phase, the desired nodes \mathbb{T}_1 and \mathbb{T}_2 transmit simultaneously, and the intermediate nodes \mathbb{R}_1 and \mathbb{R}_2 receive

$$d_1^{(1)} = h_1 x_1^{(1)} + n_1^{(1)}, \quad (1)$$

and

$$d_2^{(1)} = g_1 x_2^{(1)} + n_2^{(1)}, \quad (2)$$

respectively. $n_i^{(1)}$ represents additive white Gaussian noise (AWGN) with zero mean and σ_n^2 variance at node i , where the superscript represents the round number of data transmission. \mathbb{R}_i ($i = 1, 2$) amplifies the received signal by a fixed gain $\tilde{\alpha}_i = \sqrt{\frac{P_{r_i}}{P_i \sigma_i^2 + \sigma_n^2}}$ and broadcasts $\alpha_i d_i^{(1)}$ to its neighboring

nodes in the second phase. Then, the superimposed signal \mathbb{R}_3 received can be expressed as

$$d_3^{(1)} = \tilde{\alpha}_1 h_1 h_2 d_1^{(1)} + \tilde{\alpha}_2 g_1 g_2 d_2^{(1)} + \tilde{\alpha}_1 h_1 n_1^{(1)} + \tilde{\alpha}_2 g_2 n_2^{(1)} + n_3^{(1)}. \quad (3)$$

In order to accomplish the information exchange between the desired nodes \mathbb{T}_1 and \mathbb{T}_2 , the intermediate node \mathbb{R}_3 needs to send back the compound signal $d_3^{(1)}$ to the desired nodes, which simply reverses the forgoing data transmission process. Firstly, \mathbb{R}_3 broadcasts the scaled network coded signal $\alpha_3 d_3^{(1)}$ to \mathbb{R}_1 and \mathbb{R}_2 . At the same time, \mathbb{R}_1 and \mathbb{R}_2 also receive the new information $x_1^{(2)}$ and $x_2^{(2)}$ transmitted from the two desired nodes \mathbb{T}_1 and \mathbb{T}_2 for the second data transmission round, respectively. Then, the compound signals received at \mathbb{R}_1 and \mathbb{R}_2 in the third phase are

$$d_1^{(2)} = \underbrace{h_1 x_1^{(2)} + n_1^{(2)}}_{s_1^{(2)}} + \alpha_3 h_2 d_3^{(1)}, \quad (4)$$

$$d_2^{(2)} = \underbrace{g_1 x_2^{(2)} + n_2^{(2)}}_{s_2^{(2)}} + \alpha_3 g_2 d_3^{(1)}, \quad (5)$$

respectively, where the amplified scaling factor can be expressed as $\alpha_3 = \sqrt{\frac{P_{r3}}{P_{r1}\sigma_3^2 + P_{r2}\sigma_4^2 + \sigma_n^2}}$. The received signals at \mathbb{R}_1 or \mathbb{R}_2 consist of the new transmitted signal $x_i^{(2)}$ and the superimposed network coded signal $d_3^{(1)}$.

Next, in order to complete the first data exchange round between \mathbb{T}_1 and \mathbb{T}_2 and continue the second data transmission round simultaneously, \mathbb{R}_1 and \mathbb{R}_2 need to broadcast the amplified compound signals $d_1^{(2)}$ and $d_2^{(2)}$ to \mathbb{T}_1 , \mathbb{T}_2 and \mathbb{R}_3 . As a consequence, in the fourth phase, \mathbb{T}_1 and \mathbb{T}_2 receive

$$y_1 = \alpha_1 h_1 s_1^{(2)} + \alpha_1 \alpha_3 h_1 h_2 d_3^{(1)} + n_{y1}, \quad (6)$$

$$y_2 = \alpha_2 g_1 s_2^{(2)} + \alpha_2 \alpha_3 g_1 g_2 d_3^{(1)} + n_{y2}, \quad (7)$$

respectively. The amplified scaling factors can be represented as $\alpha_1 = \sqrt{\frac{P_{r1}}{P_1\sigma_1^2 + P_{r3}\sigma_3^2 + \sigma_n^2}}$ and $\alpha_2 = \sqrt{\frac{P_{r2}}{P_2\sigma_2^2 + P_{r3}\sigma_4^2 + \sigma_n^2}}$. As $d_3^{(1)}$ consists of the data symbols $x_1^{(1)}$ and $x_2^{(1)}$ transmitted by the desired nodes in the first round, the desired nodes can extract the data sent from others by canceling the data sent by themselves, e.g., \mathbb{T}_1 can obtain $x_2^{(1)}$ sent from \mathbb{T}_2 by deleting $x_1^{(1)}$ and $x_1^{(2)}$ transmitted by itself in the first round and second round, respectively. Meanwhile, the compound signals received at \mathbb{R}_3 are combinations of the new transmitted signal $s_3^{(2)}$ and the redundant superimposed network coded signal $d_3^{(1)}$ back from the previous round, which can be written as

$$d_3^{(2)} = \underbrace{\alpha_1 h_2 s_1^{(2)} + \alpha_2 g_2 s_2^{(2)} + n_3^{(2)}}_{s_3^{(2)}} + (\alpha_1 h_2^2 + \alpha_2 g_2^2) d_3^{(1)}. \quad (8)$$

It is inappropriate for \mathbb{R}_3 to continue broadcasting the redundant signal $d_3^{(1)}$, which results in energy dissipation due to the worthless information transmission and overlapping of the newly transmitting signal $s_3^{(2)}$. Consequently, the redundant signal $d_3^{(1)}$ is required to be removed leaving only $s_3^{(2)}$, so that the network coded data can continue to be sent

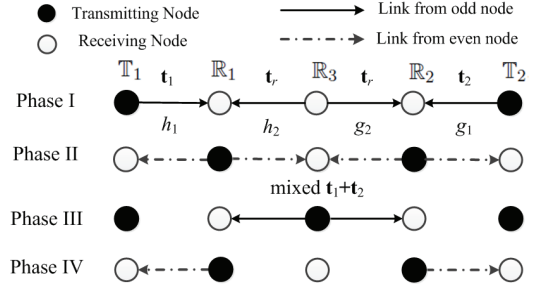


Fig. 3. Training design in 4-hop WCNs.

out. The proposed network coded transmission strategy can achieve twofold spectral efficiency performance gains over the traditional point-to-point strategy. In order to remove the redundant signal in \mathbb{R}_3 , CSI estimates \hat{h}_2 and \hat{g}_2 corresponding to h_2 and g_2 are needed, which can be acquired by standard radio channel estimation techniques. For this purpose, it is necessary to design the training process for 4-hop WCNs.

B. Training Design in 4-Hop WCNs

Considering the self-interference cancelation required at the intermediate node \mathbb{R}_3 , a completed form of the training design scheme is needed for both desired nodes and the intermediate node \mathbb{R}_3 to transmit the pilot training sequences. The training scheme should avoid the excessive consumption of resources incurred in the point-to-point scheme, where the training sequences are required for every hop. Denoting the L symbol length training sequences from \mathbb{T}_1 , \mathbb{T}_2 and \mathbb{R}_3 as \mathbf{t}_1 , \mathbf{t}_2 and \mathbf{t}_r , respectively, we further define $Q_i = \|\mathbf{t}_i\|^2$ ($i = 1, 2$) and $Q_r = \|\mathbf{t}_r\|^2$ for notational simplicity. Following the four time phases for the proposed network coding transmission strategy, each training round is divided into 4 phases as shown in Fig. 3.

In the first phase, the two desired nodes and \mathbb{R}_3 transmit simultaneously, and the received signals at \mathbb{R}_1 and \mathbb{R}_2 are expressed as

$$\mathbf{r}_1 = h_1 \mathbf{t}_1 + h_2 \mathbf{t}_r + \mathbf{n}_1^{(1)}, \quad (9)$$

$$\mathbf{r}_2 = g_1 \mathbf{t}_2 + g_2 \mathbf{t}_r + \mathbf{n}_2^{(1)}, \quad (10)$$

respectively, where $\mathbf{n}_i^{(1)}$ is the corresponding $L \times 1$ dimensional AWGN vector. Then, \mathbb{R}_i amplifies \mathbf{r}_i ($i = 1, 2$) by the fixed gain α_i and forwards $\alpha_i \mathbf{r}_i$ to its neighboring nodes in the second phase. The received training signals at \mathbb{T}_1 , \mathbb{T}_2 and \mathbb{R}_3 can be written as

$$\mathbf{z}_1 = \alpha_1 \mathbf{T}_1 \mathbf{h}_1^{(1)} + \alpha_1 h_1 \mathbf{n}_1^{(1)} + \mathbf{n}_{z1}, \quad (11)$$

$$\mathbf{z}_2 = \alpha_2 \mathbf{T}_2 \mathbf{g}_1^{(1)} + \alpha_2 g_1 \mathbf{n}_1^{(1)} + \mathbf{n}_{z2}, \quad (12)$$

$$\mathbf{r}_3 = \alpha_1 h_1 h_2 \mathbf{t}_1 + \alpha_2 g_1 g_2 \mathbf{t}_2 + (\alpha_1 h_2^2 + \alpha_2 g_2^2) \mathbf{t}_r + \tilde{\mathbf{n}}_3^{(1)}, \quad (13)$$

respectively, where $\mathbf{T}_1 = [\mathbf{t}_1, \mathbf{t}_r]$, $\mathbf{T}_2 = [\mathbf{t}_2, \mathbf{t}_r]$, $\mathbf{h}_1^{(1)} = [h_1^2, h_1 h_2]^T$, $\mathbf{g}_1^{(1)} = [g_1^2, g_1 g_2]^T$, and $\tilde{\mathbf{n}}_3^{(1)} = \alpha_1 h_2 \mathbf{n}_1^{(1)} + \alpha_2 g_2 \mathbf{n}_1^{(1)} + \mathbf{n}_3^{(1)}$. After the first training transmission round, \mathbb{T}_1 and \mathbb{T}_2 perform channel estimation to acquire $\hat{\mathbf{h}}_1^{(1)}$ and

$\hat{\mathbf{g}}_1^{(1)}$, respectively. Meanwhile, \mathbb{R}_3 needs to obtain an estimate of $\alpha_1 h_2^2 + \alpha_2 g_2^2$ for self-interference cancellation. Implementing the least squares (LS) estimation method for $\mathbf{h}_{r1} = [h_1 h_2, g_1 g_2, \alpha_1 h_2^2 + \alpha_2 g_2^2]^T$, the estimate can be written as

$$\hat{\mathbf{h}}_{r1} = \mathbf{\Lambda}_0^{-1} \mathbf{T}_r^\dagger \mathbf{r}_3 = \mathbf{h}_{r1} + \mathbf{\Lambda}_0^{-1} \mathbf{T}_r^\dagger \tilde{\mathbf{n}}_3^{(1)}, \quad (14)$$

where $\mathbf{T}_r = [\mathbf{t}_1, \mathbf{t}_2, \mathbf{t}_r]$, $\mathbf{T}_r^\dagger = (\mathbf{T}_r^H \mathbf{T}_r)^{-1} \mathbf{T}_r^H$, and $\mathbf{\Lambda}_0 = \text{diag}\{\alpha_1, \alpha_2, 1\}$.

Since \mathbf{t}_r is useless for the channel estimation at the desired nodes, the training signals transmitted in the third phase only retain \mathbf{t}_1 and \mathbf{t}_2 . The corresponding channel parameters can be written as $\mathbf{h}_r = [h_1 h_2, g_1 g_2]$. In this case, \mathbb{R}_3 broadcasts the re-organized training signals based on LS estimation, which can be expressed as

$$\tilde{\mathbf{r}}_3 = \tilde{\alpha}_3 \mathbf{T} \mathbf{\Lambda} \hat{\mathbf{h}}_r = \tilde{\alpha}_3 (\alpha_1 h_1 h_2 \mathbf{t}_1 + \alpha_2 g_1 g_2 \mathbf{t}_2 + \tilde{\mathbf{n}}_r), \quad (15)$$

where $\mathbf{T} = [\mathbf{t}_1, \mathbf{t}_2]$, and $\mathbf{\Lambda} = \text{diag}\{\alpha_1, \alpha_2\}$. $\tilde{\mathbf{n}}_r = \mathbf{T} (\mathbf{T}^H \mathbf{T})^{-1} \mathbf{T}^H \tilde{\mathbf{n}}_3^{(1)}$ is the LS estimation error, which can be regarded as the residual noise.

The total noise power can be calculated as

$$\mathcal{E} \{ \tilde{\mathbf{n}}_r^H \tilde{\mathbf{n}}_r \} = 2 (\alpha_1^2 \sigma_3^2 + \alpha_2^2 \sigma_4^2 + 1) \sigma_n^2. \quad (16)$$

The parameter $\tilde{\alpha}_3$ can be explicitly written as

$$\tilde{\alpha}_3 = \sqrt{\frac{LP_r}{\alpha_1 \sigma_1^2 \sigma_3^2 LP_1 + \alpha_2 \sigma_2^2 \sigma_4^2 LP_2 + 2 (\alpha_1^2 \sigma_3^2 + \alpha_2^2 \sigma_4^2 + 1) \sigma_n^2}}. \quad (17)$$

Finally, the received signal at \mathbb{T}_1 can be expressed as

$$\mathbf{z}_3 = \alpha_1 h_1 h_2 \tilde{\mathbf{r}}_3 + \tilde{\mathbf{n}}_{z_3}, \quad (18)$$

where $\tilde{\mathbf{n}}_{z_3} = \alpha_1 h_1 \mathbf{n}_1^{(2)} + \mathbf{n}_{z_3}$ is the $L \times 1$ dimensional equivalent noise vector.

By substituting (15) into (18), \mathbf{z}_3 can be rewritten as

$$\mathbf{z}_3 = \alpha_1 \tilde{\alpha}_3 \mathbf{T} \mathbf{\Lambda} \boldsymbol{\theta} + \tilde{\mathbf{n}}, \quad (19)$$

where $\boldsymbol{\theta} = [h_1^2 h_2^2, h_1 h_2 g_1 g_2]^T$ and $\tilde{\mathbf{n}} = \alpha_1 \tilde{\alpha}_3 h_1 h_2 \tilde{\mathbf{n}}_r^{(1)} + \alpha_1 h_1 \mathbf{n}_1^{(2)} + \mathbf{n}_{z_3}$.

III. CHANNEL ESTIMATION FOR 4-HOP WCNs

In this section, both LMMSE and ML estimation schemes are analyzed to obtain radio channel coefficients at each node in 4-hop WCNs. The correlation coefficient between the training sequences \mathbf{t}_1 and \mathbf{t}_2 sent by \mathbb{T}_1 and \mathbb{T}_2 , respectively, can be written as $\rho = \mathbf{t}_1^H \mathbf{t}_2 / \sqrt{Q_1 Q_2}$.

A. LMMSE Channel Estimation Scheme

The second order statistics σ_i^2 ($i = 1, \dots, 4$) and σ_n^2 are assumed to be known by the transmitters. Following the standard approach in [23], according to the received training signal in (19), the radio channel $\boldsymbol{\theta}$ can be estimated as $\hat{\boldsymbol{\theta}}$ via LMMSE estimation, and $\hat{\boldsymbol{\theta}}$ can be directly derived as

$$\hat{\boldsymbol{\theta}} = \mathcal{E} \{ \boldsymbol{\theta} \mathbf{z}_3^H \} (\mathcal{E} \{ \mathbf{z}_3 \mathbf{z}_3^H \})^{-1} \mathbf{z}_3. \quad (20)$$

Substituting (19) into (20), the radio channel estimate can be re-expressed as

$$\hat{\boldsymbol{\theta}} = \alpha_1 \tilde{\alpha}_3 \mathbf{R}_\theta \mathbf{\Lambda} \mathbf{T}^H (\alpha_1^2 \tilde{\alpha}_3^2 \mathbf{T} \mathbf{\Lambda} \mathbf{R}_\theta \mathbf{\Lambda} \mathbf{T}^H + \mathbf{R}_{\tilde{\mathbf{n}}})^{-1} \mathbf{z}_3, \quad (21)$$

where $\mathbf{R}_\theta = \mathcal{E} \{ \boldsymbol{\theta} \boldsymbol{\theta}^H \} = \text{diag} \left\{ \underbrace{4\sigma_1^4 \sigma_3^4}_{\sigma_{\theta_1}^2}, \underbrace{\sigma_1^2 \sigma_2^2 \sigma_3^2 \sigma_4^2}_{\sigma_{\theta_2}^2} \right\}$.

The corresponding MSE is given by

$$\sigma_\theta^2 = \text{tr} \{ (\mathbf{R}_\theta^{-1} + \alpha_1^2 \tilde{\alpha}_3^2 \mathbf{\Lambda} \mathbf{T}^H \mathbf{R}_{\tilde{\mathbf{n}}}^{-1} \mathbf{T} \mathbf{\Lambda})^{-1} \}, \quad (22)$$

where the covariance matrix of the equivalent noise is $\mathbf{R}_{\tilde{\mathbf{n}}} = \sigma_n^2 (\xi \mathbf{I}_N + \alpha_1^2 \tilde{\alpha}_3^2 \sigma_1^2 \sigma_3^2 \varepsilon \mathbf{T} (\mathbf{T}^H \mathbf{T})^{-1} \mathbf{T}^H)$. To simplify notation, we can define $\varepsilon = (2\alpha_1^2 \sigma_3^2 + \alpha_2^2 \sigma_4^2 + 1)$, and $\xi = (1 + \alpha_1^2 \sigma_1^2)$. By substituting the equivalent noise covariance matrix $\mathbf{R}_{\tilde{\mathbf{n}}}$ into \mathbf{R}_{z_3} , the explicit expression of \mathbf{R}_{z_3} can be written in

$$\mathbf{R}_{z_3} = \sigma_n^2 \xi (\mathbf{I}_N + A_1 \mathbf{t}_1 \mathbf{t}_1^H + A_2 \mathbf{t}_2 \mathbf{t}_2^H + A_3 \mathbf{t}_1 \mathbf{t}_2^H + A_3^* \mathbf{t}_2 \mathbf{t}_1^H), \quad (23)$$

where $A_1 = \frac{\alpha_1^2 \tilde{\alpha}_3^2}{\xi} \left(\frac{\alpha_1 \sigma_{\theta_1}^2}{\sigma_n^2} + \frac{\sigma_1^2 \sigma_3^2 \varepsilon}{(1-|\rho|^2) Q_1} \right)$, $A_2 = \frac{\alpha_2^2 \tilde{\alpha}_3^2}{\xi} \left(\frac{\alpha_2 \sigma_{\theta_2}^2}{\sigma_n^2} + \frac{\sigma_1^2 \sigma_3^2 \varepsilon}{(1-|\rho|^2) Q_2} \right)$, and $A_3 = -\alpha_1^2 \tilde{\alpha}_3^2 \frac{\rho \sigma_1^2 \sigma_3^2 \varepsilon}{(1-|\rho|^2) \sqrt{Q_1 Q_2} \xi}$.

By expanding (21), $\hat{\theta}_1$ and $\hat{\theta}_2$ can be estimated respectively as

$$\hat{\theta}_1 = \alpha_1^2 \tilde{\alpha}_3 \sigma_{\theta_1}^2 \mathbf{t}_1^H \mathbf{R}_{z_3}^{-1} \mathbf{z}_3, \quad (24)$$

$$\hat{\theta}_2 = \alpha_1 \alpha_2 \tilde{\alpha}_3 \sigma_{\theta_2}^2 \mathbf{t}_2^H \mathbf{R}_{z_3}^{-1} \mathbf{z}_3. \quad (25)$$

By substituting (23) into (24) and (25), the corresponding channel estimates can be rewritten as

$$\hat{\theta}_1 = \frac{\alpha_1^2 \tilde{\alpha}_3 \sigma_{\theta_1}^2}{\tau \xi \sigma_n^2} [(1 + A_2 Q_2 + A_3^* \rho \sqrt{Q_1 Q_2}) \mathbf{t}_1^H - (A_3^* Q_1 + A_2 \rho^* \sqrt{Q_1 Q_2} \mathbf{t}_2^H)] \mathbf{z}_3, \quad (26)$$

$$\hat{\theta}_2 = \frac{\alpha_1 \alpha_2 \tilde{\alpha}_3 \sigma_{\theta_2}^2}{\tau \xi \sigma_n^2} [(1 + A_1 Q_1 + A_3^* \rho \sqrt{Q_1 Q_2}) \mathbf{t}_2^H - (A_3 Q_2 + A_1 \rho \sqrt{Q_1 Q_2} \mathbf{t}_1^H)] \mathbf{z}_3, \quad (27)$$

where $\tau = 1 + A_1 Q_1 + A_2 Q_2 + 2A_3 \rho^* \sqrt{Q_1 Q_2} + (A_1 A_2 - |A_3|^2) Q_1 Q_2$.

The MSEs of θ_1 and θ_2 are defined as e_{θ_1} and e_{θ_2} , respectively, as shown in

$$e_{\theta_1} = \mathcal{E} \{ |\Delta_a|^2 \} = \sigma_{\theta_1}^2 - \alpha_1^4 \tilde{\alpha}_3^2 \sigma_{\theta_1}^4 \mathbf{t}_1^H \mathbf{R}_{z_3}^{-1} \mathbf{t}_1, \quad (28)$$

$$e_{\theta_2} = \mathcal{E} \{ |\Delta_b|^2 \} = \sigma_{\theta_2}^2 - \alpha_1^2 \alpha_2^2 \tilde{\alpha}_3^2 \sigma_{\theta_2}^4 \mathbf{t}_2^H \mathbf{R}_{z_3}^{-1} \mathbf{t}_2. \quad (29)$$

Similarly, the quantities $\mathbf{t}_1^H \mathbf{R}_{z_3}^{-1} \mathbf{t}_1$ and $\mathbf{t}_2^H \mathbf{R}_{z_3}^{-1} \mathbf{t}_2$ can be written as

$$\mathbf{t}_1^H \mathbf{R}_{z_3}^{-1} \mathbf{t}_1 = \frac{Q_1 + A_2 (1 - |\rho|^2) Q_1 Q_2}{\tau \xi \sigma_n^2}, \quad (30)$$

$$\mathbf{t}_2^H \mathbf{R}_{z_3}^{-1} \mathbf{t}_2 = \frac{Q_2 + A_1 (1 - |\rho|^2) Q_1 Q_2}{\tau \xi \sigma_n^2}. \quad (31)$$

B. ML Estimation Scheme

Although LMMSE estimation has low complexity, the second order channel statistics of every hop are often not available at all nodes. Therefore, ML is studied in this paper to provide potential solutions to this problem by assuming the radio channels to be *deterministic*. To apply ML, the probability density function (pdf) of \mathbf{z}_3 can be written as

$$p(\mathbf{z}_3|\theta) = \pi^{-N} |\mathbf{R}_{\hat{\mathbf{n}}}|^{-1} \exp(-(\mathbf{z}_3 - \alpha_1 \tilde{\alpha}_3 \mathbf{T} \Lambda \theta)^H \mathbf{R}_{\hat{\mathbf{n}}}^{-1} (\mathbf{z}_3 - \alpha_1 \tilde{\alpha}_3 \mathbf{T} \Lambda \theta)). \quad (32)$$

The log-likelihood function is thus given by

$$\log p(\mathbf{z}_3|\theta) = -(\mathbf{z}_3 - \alpha_1 \tilde{\alpha}_3 \mathbf{T} \Lambda \theta)^H \mathbf{R}_{\hat{\mathbf{n}}}^{-1} (\mathbf{z}_3 - \alpha_1 \tilde{\alpha}_3 \mathbf{T} \Lambda \theta) - \log(|\mathbf{R}_{\hat{\mathbf{n}}}|) - N \log(\pi). \quad (33)$$

By maximizing (33), ML estimates of θ_1 and θ_2 can be obtained from

$$\{\hat{\theta}_1, \hat{\theta}_2\} = \arg \min_{\theta_1, \theta_2} (\mathbf{z}_3 - \alpha_1^2 \tilde{\alpha}_3 \theta_1 \mathbf{t}_1 - \alpha_1 \alpha_2 \tilde{\alpha}_3 \theta_2 \mathbf{t}_2)^H \mathbf{R}_{\hat{\mathbf{n}}}^{-1} (\mathbf{z}_3 - \alpha_1^2 \tilde{\alpha}_3 \theta_1 \mathbf{t}_1 - \alpha_1 \alpha_2 \tilde{\alpha}_3 \theta_2 \mathbf{t}_2) + \log(|\mathbf{R}_{\hat{\mathbf{n}}}|). \quad (34)$$

$\mathbf{R}_{\hat{\mathbf{n}}}$ can be expressed explicitly as

$$\begin{aligned} \mathbf{R}_{\hat{\mathbf{n}}} &= \sigma_n^2 (\xi \mathbf{I}_N + \alpha_1^2 \tilde{\alpha}_3 |\theta_1| \varepsilon \mathbf{T} (\mathbf{T}^H \mathbf{T})^{-1} \mathbf{T}^H) \\ &= \sigma_n^2 \xi (\mathbf{I}_N + a \mathbf{P}_T), \end{aligned} \quad (35)$$

where \mathbf{P}_T is the projection matrix of the space spanned by the training matrix \mathbf{T} , and $a = \frac{\alpha_1^2 \tilde{\alpha}_3^2 \varepsilon}{\xi} |\theta_1|$. As the estimate $\hat{\theta}_2$ is independent of the second term in (34), we can obtain $\hat{\theta}_2$ simply from the least-squares approach under a given θ_1 as

$$\begin{aligned} \hat{\theta}_2 &= \arg \min_{\theta_2} (-(\mathbf{z}_3 - \alpha_1^2 \tilde{\alpha}_3 \theta_1 \mathbf{t}_1 - \alpha_1 \alpha_2 \tilde{\alpha}_3 \theta_2 \mathbf{t}_2)^H \\ &\mathbf{R}_{\hat{\mathbf{n}}}^{-1} (\mathbf{z}_3 - \alpha_1^2 \tilde{\alpha}_3 \theta_1 \mathbf{t}_1 - \alpha_1 \alpha_2 \tilde{\alpha}_3 \theta_2 \mathbf{t}_2)). \end{aligned} \quad (36)$$

Consequently, $\hat{\theta}_2$ can be written as

$$\hat{\theta}_2 = \frac{\mathbf{t}_2^H \mathbf{R}_{\hat{\mathbf{n}}}^{-1}}{\alpha_1 \alpha_2 \tilde{\alpha}_3 \mathbf{t}_2^H \mathbf{R}_{\hat{\mathbf{n}}}^{-1} \mathbf{t}_2} (\mathbf{z}_3 - \alpha_1^2 \tilde{\alpha}_3 \theta_1 \mathbf{t}_1). \quad (37)$$

As the inverse of the equivalent noise is $\mathbf{R}_{\hat{\mathbf{n}}}^{-1} = \frac{1}{\sigma_n^2 \xi} (\mathbf{I} - \frac{a}{1+a} \mathbf{P}_T)$, $\hat{\theta}_2$ can be further simplified to

$$\hat{\theta}_2 = \frac{\mathbf{t}_2^H}{\alpha_1 \alpha_2 \tilde{\alpha}_3 Q_2} (\mathbf{z}_3 - \alpha_1^2 \tilde{\alpha}_3 \theta_1 \mathbf{t}_1). \quad (38)$$

By substituting $\hat{\theta}_2$ back into (34), the log-likelihood function can be reformulated as

$$\begin{aligned} \hat{\theta}_1 &= \arg \min_h \left\{ \mathbf{z}_3^H \mathbf{B} \mathbf{z}_3 - 2\alpha_1^2 \tilde{\alpha}_3 \Re \{ \theta_1 \mathbf{z}_3^H \mathbf{B} \mathbf{z}_3 \} \right. \\ &\left. + \alpha_1^4 \alpha_3^2 |\theta_1|^2 \mathbf{t}_1^H \mathbf{B} \mathbf{t}_1 + \log(|\mathbf{R}_{\hat{\mathbf{n}}}|) \right\}, \end{aligned} \quad (39)$$

where $\mathbf{A} = \mathbf{I} - \frac{\mathbf{t}_2 \mathbf{t}_2^H \mathbf{R}_{\hat{\mathbf{n}}}^{-1}}{\mathbf{t}_2^H \mathbf{R}_{\hat{\mathbf{n}}}^{-1} \mathbf{t}_2}$, and

$$\mathbf{B} \triangleq \mathbf{A}^H \mathbf{R}_{\hat{\mathbf{n}}}^{-1} \mathbf{A} = \left(\mathbf{R}_{\hat{\mathbf{n}}}^{-1} - \frac{\mathbf{R}_{\hat{\mathbf{n}}}^{-1} \mathbf{t}_2 \mathbf{t}_2^H \mathbf{R}_{\hat{\mathbf{n}}}^{-1}}{\mathbf{t}_2^H \mathbf{R}_{\hat{\mathbf{n}}}^{-1} \mathbf{t}_2} \right). \quad (40)$$

Since \mathbf{B} and the determinant of $\mathbf{R}_{\hat{\mathbf{n}}}$ contain only the amplitude $|\theta_1|$, the phase $\angle \theta_1$ of θ_1 can be independently estimated as

$$\widehat{\angle \theta}_1 = -\angle(\mathbf{z}_3^H \mathbf{B} \mathbf{t}_1). \quad (41)$$

By minimizing the expression in (34), $|\theta_1|$ can be estimated as

$$\begin{aligned} \widehat{|\theta_1|} &= \arg \min_{|\theta_1|} \underbrace{\mathbf{z}_3^H \mathbf{B} \mathbf{z}_3 - 2\alpha_1^2 \tilde{\alpha}_3 |\theta_1| |\mathbf{z}_3^H \mathbf{B} \mathbf{t}_1| + \alpha_1^4 \tilde{\alpha}_3^2 |\theta_1|^2 \mathbf{t}_1^H \mathbf{B} \mathbf{t}_1}_{f_1(a)} + \\ &\log(|\mathbf{R}_{\hat{\mathbf{n}}}|), \end{aligned} \quad (42)$$

$$\begin{aligned} &= \arg \min_{|\theta_1|} \underbrace{\mathbf{z}_3^H \mathbf{B} \mathbf{z}_3 - 2 \frac{\alpha_1^2 \tilde{\alpha}_3 a}{a_0} |\mathbf{z}_3^H \mathbf{B} \mathbf{t}_1| + \left(\frac{\alpha_1^2 \tilde{\alpha}_3 a}{a_0} \right)^2 \mathbf{t}_1^H \mathbf{B} \mathbf{t}_1}_{f_1(a)} + \\ &\log(|\mathbf{R}_{\hat{\mathbf{n}}}|). \end{aligned} \quad (43)$$

Considering that $a = a_0 |\theta_1|$ is a simple multiple factor of the estimate $|\theta_1|$ with $a_0 = \frac{\alpha_1^2 \tilde{\alpha}_3^2 \varepsilon}{\xi}$, the minimization of (42) in terms of $|\theta_1|$ can be solved via searching the corresponding a . Then, the derivative of the first part $f_1(a)$ in (43) with respect to a can be expressed as

$$\begin{aligned} \dot{f}_1(a) &= \frac{\partial f_1(a)}{\partial a} = \mathbf{z}_3^H \frac{\partial \mathbf{B}}{\partial a} \mathbf{z}_3 - 2 \frac{\alpha_1^2 \tilde{\alpha}_3}{a_0} \frac{\partial (a |\mathbf{z}_3^H \mathbf{B} \mathbf{t}_1|)}{\partial a} \\ &+ \left(\frac{\alpha_1^2 \tilde{\alpha}_3}{a_0} \right)^2 \mathbf{t}_1^H \frac{\partial (a^2 \mathbf{B})}{\partial a} \mathbf{t}_1. \end{aligned} \quad (44)$$

According to the definition of the matrix \mathbf{B} in (40), the derivative of \mathbf{B} with respect to a can be expressed as

$$\frac{\partial \mathbf{B}}{\partial a} = \frac{1}{\sigma_n^2 \xi (1+a)^2} \left(-\mathbf{P}_T + \frac{1}{Q_2} \mathbf{t}_2 \mathbf{t}_2^H \right). \quad (45)$$

In order to obtain an analytical solution for a , the specific form of $|\mathbf{z}_3^H \mathbf{B} \mathbf{t}_1|$ in (44) can be rewritten as

$$|\mathbf{z}_3^H \mathbf{B} \mathbf{t}_1| = \frac{1}{\sigma_n^2 \xi (1+a)} |\mathbf{z}_3^H \mathbf{t}_1 - \rho^* \sqrt{Q_1/Q_2} \mathbf{z}_3^H \mathbf{t}_2|. \quad (46)$$

The estimated phase $\widehat{\angle \theta}_1$ for $|\mathbf{z}_3^H \mathbf{B} \mathbf{t}_1|$ in (46) is re-expressed as

$$\widehat{\angle \theta}_1 = -\angle(\mathbf{z}_3^H \mathbf{B} \mathbf{t}_1) = -\angle\left(\mathbf{z}_3^H \mathbf{t}_1 - \rho^* \sqrt{Q_1/Q_2} \mathbf{z}_3^H \mathbf{t}_2\right), \quad (47)$$

which indicates that $\widehat{\angle \theta}_1$ is independent of $|\theta_1|$.

Similarly, the derivation of the other items of $\dot{f}_1(a)$ in (44) is directly given by $\mathbf{t}_1^H \mathbf{B} \mathbf{t}_1 = \frac{1-\rho^2}{1+a} Q_1$, and $\mathbf{z}_3^H \frac{\partial \mathbf{B}}{\partial a} \mathbf{z}_3 = \frac{1}{\sigma_n^2 \xi (1+a)^2} \left(-\mathbf{z}_3^H \mathbf{P}_T \mathbf{z}_3 + \frac{1}{Q_2} |\mathbf{z}_3^H \mathbf{t}_2|^2 \right)$. Therefore, the derivative of $f_1(a)$ can be re-organized as

$$\begin{aligned} \dot{f}_1(a) &= \frac{1}{\sigma_n^2 \xi (1+a)^2} \left[\left(-\mathbf{z}_3^H \mathbf{P}_T \mathbf{z}_3 + \frac{1}{Q_2} |\mathbf{z}_3^H \mathbf{t}_2|^2 \right) \right. \\ &- 2 \frac{\alpha_1^2 \tilde{\alpha}_3}{a_0} |\mathbf{z}_3^H \mathbf{t}_1 - \rho^* \sqrt{Q_1/Q_2} \mathbf{z}_3^H \mathbf{t}_2| \\ &\left. + \frac{\alpha_1^4 \tilde{\alpha}_3^2}{a_0^2} (2a + a^2) (1 - \rho^2) Q_1 \right]. \end{aligned} \quad (48)$$

The remaining part of (43) is to calculate the derivative of $\log(|\mathbf{R}_{\hat{\mathbf{n}}}|)$. Since \mathbf{P}_T is an orthogonal projection matrix, both

\mathbf{I} and \mathbf{P}_T are symmetric matrices. We can define $f_2(a) = \log \det(\mathbf{I} + a\mathbf{P}_T)$, which can be transformed into

$$f_2(a) = \sum_{i=1}^N \log(1 + a\lambda_i), \quad (49)$$

where λ_i is the eigenvalue of the projection matrix \mathbf{P}_T .

The derivative of $\log(|\mathbf{R}_{\tilde{\mathbf{n}}}|)$ with respect to a is equal to $\dot{f}_2(a)$, which can be expressed as

$$\dot{f}_2(a) = \sum_{i=1}^N \frac{\lambda_i}{1 + a\lambda_i}. \quad (50)$$

The eigenvalue projection matrix \mathbf{P}_T is only 0 or 1, and the number of such that $\lambda_i = 1$ is equal to the rank of \mathbf{P}_T . The projection matrix satisfies $\text{tr}\{\mathbf{P}_T\} = \text{rank}(\mathbf{P}_T)$. Therefore, $\dot{f}_2(a)$ is given by

$$\dot{f}_2(a) = \frac{r}{1+a}, \quad (51)$$

where $r = \text{tr}\{\mathbf{P}_T\}$. Denoting by $f(a)$ the objective function in (43) and substituting the derivatives obtained in (51) into $\dot{f}(a)$, the derivative of $f(a)$ can be expressed concisely as

$$\dot{f}(a) = \frac{C_1 a^2 + C_2 a + C_3}{\sigma_n^2 \xi a_0^2 (1+a)^2}, \quad (52)$$

where $C_1 = \alpha_1^4 \tilde{\alpha}_3^2 (1 - |\rho|^2) Q_1$, $C_2 = 2\alpha_1^4 \tilde{\alpha}_3^2 (1 - |\rho|^2) Q_1 + r a_0^2 \sigma_n^2 \xi$, and $C_3 = a_0^2 \left(-\mathbf{z}_3^H \mathbf{P}_T \mathbf{z}_3 + \frac{1}{Q_2} |\mathbf{z}_3^H \mathbf{t}_2|^2 \right) - 2\alpha_1^2 \tilde{\alpha}_3 a_0 |\mathbf{z}_3^H \mathbf{t}_1 - \rho^* \sqrt{Q_1/Q_2} \mathbf{z}_3^H \mathbf{t}_2| + r a_0^2 \sigma_n^2 \xi$.

Depending on the value of $|\rho|$, the coefficient C_1 is larger than or equal to zero. The solution to the above equation can be obtained in the following two cases.

Case I: When $|\rho| = 1$, \mathbf{t}_1 and \mathbf{t}_2 are fully correlated and $C_1 = 0$, the solution can be obtained as $a = -\frac{C_3}{C_2}$ is straightforward. If the coefficient C_2 is larger than zero owing to $r > 0$, the solution $a = -\frac{C_3}{C_2}$ is the global minimum of $f(a)$. Considering that $a \geq 0$, the estimate of a is given by

$$\hat{a} = \max\{-C_3/C_2, 0\}. \quad (53)$$

In practice, designing fully correlated training is inadvisable since the two channel parameters θ_1 and θ_2 would then be indistinguishable.

Case II: When $|\rho| < 1$ and $C_1 > 0$, \mathbf{t}_1 and \mathbf{t}_2 are partially correlated or even orthogonal. The root of the quadratic function $\dot{f}(a)$ is determined by the discriminant $C_2^2 - 4C_1C_3$. When $C_2^2 - 4C_1C_3 \geq 0$, the two roots of $\dot{f}(a)$ can be written in $a_{1,2} = \frac{-C_2 \pm \sqrt{C_2^2 - 4C_1C_3}}{2C_1}$. It is readily affirmed that $a_1 = \frac{-C_2 - \sqrt{C_2^2 - 4C_1C_3}}{2C_1}$ must be a local maximum, and $a_2 = \frac{-C_2 + \sqrt{C_2^2 - 4C_1C_3}}{2C_1}$ must be a local minimum due to the fact that $C_1 > 0$. Considering $a \geq 0$, the estimate of a is simply expressed as

$$\hat{a} = \max\left\{ \frac{-C_2 + \sqrt{C_2^2 - 4C_1C_3}}{2C_1}, 0 \right\}. \quad (54)$$

When the discriminant $C_2^2 - 4C_1C_3 < 0$, $\dot{f}(a)$ has no roots and $f(a)$ is a monotonically increasing function. As a consequence, the estimate is simply $\hat{a} = 0$ where the minimum of $f(a)$ lies. Once the estimate of a is obtained, the corresponding $|\theta_1|$ can be calculated from $|\theta_1| = a/a_0$.

IV. TRAINING DESIGN FOR 4-HOP WCNS

In this section, based on the channel estimation schemes proposed in Section III, the corresponding optimal training designs obtained by minimizing MSE for LMMSE estimation are characterized in the following lemmas and proposition.

Lemma 1: The optimal LMMSE-based training in 4-hop WCNS is orthogonal with maximum allowable transmit power.

Proof: See Appendix A. ■

Due to the nonlinearity of ML, it is difficult to obtain a closed-form expression of the corresponding MSE, and the training design method for LMMSE estimation based on minimizing MSE is not suitable. Instead, we resort to designing training sequences from minimizing the Cramér Rao Lower Bound (CRLB), which provides a lower bound on the variance of unbiased estimates.

Proposition 2: The CRLBs for θ in 4-hop WCNS are

$$\text{CRLB}_{\theta_1} = \frac{D_3(D_1 D_3 - |D_2|^2)}{|D_2|^4 - 2D_1 D_3 |D_2|^2 + D_1^2 D_3^2 - |D_4|^2 D_3^2}, \quad (55)$$

$$\text{CRLB}_{\theta_2} = \frac{(-D_1 |D_2|^2 - |D_4|^2 D_3 + D_1^2 D_3)}{|D_2|^4 - 2D_1 D_3 |D_2|^2 + D_1^2 D_3^2 - |D_4|^2 D_3^2}, \quad (56)$$

where

$$D_1 = \frac{\alpha_1^4 \tilde{\alpha}_3^2 Q_1}{\sigma_n^2 \xi (1+a)} + \frac{a_0^2 (r-2)^2}{4(1+a)^2}, \quad D_2 = \frac{\alpha_1^4 \tilde{\alpha}_3^2 \rho \sqrt{Q_1 Q_2}}{\sigma_n^2 \xi (1+a)},$$

$$D_3 = \frac{\alpha_1^4 \tilde{\alpha}_3^2 Q_2}{\sigma_n^2 \xi (1+a)}, \quad D_4 = \frac{a_0^2 (r-2)^2 \theta_1^2}{4(1+a)^2 |\theta_1|^2}.$$

Proof: See Appendix B. ■

Once the explicit forms of CRLB_{θ_1} and CRLB_{θ_2} are obtained, optimal training design by minimizing CRLBs can be developed according to the following lemma.

Lemma 3: The optimal training design based on minimizing the CRLB is orthogonal with maximum allowable transmit power.

Proof: See Appendix C. ■

V. GENERAL NETWORK CODED 2N-HOP WCNS

In this section, the network coding transmission strategy, radio channel estimation and corresponding training design schemes for general MH-WCNS are considered as extensions of 4-hop WCNS. The $2N$ -hop WCNS are bidirectional multi-hop networks with $2N - 1$ cascaded cooperative intermediate nodes \mathbb{R}_{2n-1} , $n = 1, \dots, N$ ($N \geq 2$) and two desired nodes \mathbb{T}_1 and \mathbb{T}_2 . The average transmission power of \mathbb{T}_i ($i = 1, 2$) and \mathbb{R}_i ($i = 1, 2, \dots, 2N - 1$) are set as P_i and P_{r_i} , respectively. The radio channels are reciprocal as time-division-duplex (TDD) is utilized. Denote the radio channel gain from \mathbb{T}_1 to \mathbb{R}_1 as h_1 , from \mathbb{T}_2 to \mathbb{R}_2 as g_1 , from \mathbb{R}_{2N-3} to \mathbb{R}_{2N-1} as h_N , and from \mathbb{R}_{2N-4} to \mathbb{R}_{2N-2} as g_N . In addition, the radio channel gain between \mathbb{R}_{2i-3} and \mathbb{R}_{2i-1} is denoted by h_i , and that between \mathbb{R}_{2i-2} and \mathbb{R}_{2i} is denoted by g_i . All radio channels satisfy $h_i \sim \mathcal{CN}(0, \sigma_{2i-1}^2)$, and $g_i \sim \mathcal{CN}(0, \sigma_{2i}^2)$, $i = 1, \dots, N$.

A. Network Coding Transmission Strategy in $2N$ -Hop WCNs

Analogously to the network coding transmission strategy in 4-hop WCNs, the signals $x_1^{(1)}$ and $x_2^{(1)}$ transmitted by two desired nodes in $2N$ -hop WCNs are exchanged in $2N$ time phases, with nearly every node required to eliminate self-interference. The signal received at \mathbb{T}_1 is

$$\begin{aligned} d_1 &= \alpha_1 h_1 s_1^{(N)} + \alpha_1 \alpha_3 h_1 h_2 s_3^{(N-1)} + \dots + \\ &\left(\prod_{i=1}^N \alpha_{2i-1} h_i \right) s_{2N-1}^{(1)} + n_1 \\ &= \left[\sum_{j=1}^N \left(\prod_{i=1}^j \alpha_{2i-1} h_i \right) s_{2j-1}^{(N+1-j)} \right] + n_1 \end{aligned} \quad (57)$$

Similarly, the signal received at \mathbb{T}_2 is given by

$$\begin{aligned} d_2 &= \left[\sum_{j=1}^{N-1} \left(\prod_{i=1}^j \alpha_{2i} g_i \right) s_{2j}^{(N+1-j)} \right] \\ &+ \alpha_{2N-1} \left(\prod_{i=1}^{N-1} \alpha_{2i} g_i \right) g_N s_{2N-1}^{(1)} + n_2 \end{aligned} \quad (58)$$

where

$$\begin{aligned} s_{2j-1}^{(N+1-j)} &= \left(\prod_{p=1}^{j-1} \alpha_{2p-1} h_{p+1} \right) h_1 x_1^{(N+1-j)} + n_{2j-1}^{(N+1-j)} \\ &+ \left[\sum_{p=1}^{j-1} \left(\prod_{q=p}^{j-1} \alpha_{2q-1} h_{q+1} \right) n_{2p-1}^{(N+1-j)} \right], \\ s_{2j}^{(N+1-j)} &= \left(\prod_{p=1}^{j-1} \alpha_{2p} g_{p+1} \right) g_1 x_2^{(N+1-j)} + n_{2j}^{(N+1-j)} \\ &+ \left[\sum_{p=1}^{j-1} \left(\prod_{q=p}^{j-1} \alpha_{2q} g_{q+1} \right) n_{2p}^{(N+1-j)} \right], \end{aligned}$$

$$\begin{aligned} \alpha_{2i-1} &= \sqrt{\frac{P_r(2i-1)}{P_r(2i-3)\sigma_{2i-3}^2 + P_r(2i+1)\sigma_{2i+2}^2 + \sigma_n^2}}, \\ \alpha_{2i} &= \sqrt{\frac{P_r(2i)}{P_r(2i-2)\sigma_{2i-2}^2 + P_r(2i+2)\sigma_{2i+2}^2 + \sigma_n^2}}, \\ i &= 2, 3, \dots, N-1, j = 2, \dots, N-1, \end{aligned}$$

$$\begin{aligned} s_1^{(N)} &= h_1 x_1^{(N)} + n_1^{(N)}, \quad s_2^{(N)} = g_1 x_2^{(N)} + n_2^{(N)}, \\ s_{2N-1}^{(1)} &= \alpha_{2N-3} h_N s_{2N-3}^{(1)} + \alpha_{2N-2} g_N s_{2N-2}^{(1)} + n_{2N-1}^{(1)}. \end{aligned}$$

The target information for \mathbb{T}_1 in (57) is $x_2^{(1)}$ transmitted from \mathbb{T}_2 . The other terms are the self-interference $x_1^{(1)}, x_1^{(2)}, \dots, x_1^{(N)}$ induced by the network coding transmission strategy and the Gaussian noise generated by the nodes during the transmission. By designing the training process meticulously, $x_2^{(1)}$ can be extracted at \mathbb{T}_1 by the corresponding channel estimation scheme. Moreover, not only does signal detection at the desired nodes need radio channel estimation, but the other intermediate nodes also need the corresponding radio channel coefficients to suppress the self-interference and make the network coding transmission strategy feasible. For instance, the received signals at the nodes $\mathbb{R}_{2i-1}, i=2, 4, \dots$ on the left-hand side of \mathbb{R}_{2N-1} when \mathbb{T}_1 receives $x_2^{(1)}$ are

$$\begin{aligned} d_{2i-1} &= s_{2i-1}^{(N-i+2)} + \sum_{j=i+1}^N \left(\prod_{m=i+1}^j \alpha_{2m-1} h_m \right) \\ &s_{2j-1}^{(N-j+2)} + \alpha_{2j-3} \alpha_{2j-1} h_j^2 \\ &\left[\sum_{j=i+1}^N \left(\prod_{m=i+1}^j \alpha_{2m-1} h_m \right) s_{2j-1}^{(N-j+1)} + s_{2i-1}^{(N-i+1)} \right], \end{aligned} \quad (59)$$

where $\sum_{j=i+1}^N \left(\prod_{m=i+1}^j \alpha_{2m-1} h_m \right) s_{2j-1}^{(N-j+1)} + s_{2i-1}^{(N-i+1)}$ is the network coded signal that \mathbb{R}_{2i-1} receives at the previous round, which is the self-interference to be deleted by \mathbb{R}_{2i-1} through estimating h_j^2 . Similarly, the nodes $\mathbb{R}_{2i-2}, i=2, 4, \dots$ located on the right-hand side of \mathbb{R}_{2N-1} should estimate g_j^2 for the interference cancellation. Therefore, the training process design in $2N$ -hop WCNs should satisfy the above-mentioned requirements, which is similar to the training design in 4-hop WCNs.

B. Training Design in $2N$ -Hop WCNs

Like the 4-hop scenario, the desired nodes \mathbb{T}_1 and \mathbb{T}_2 in $2N$ -hop WCNs send \mathbf{t}_1 and \mathbf{t}_2 , and the intermediate node \mathbb{R}_{2N-1} transmits \mathbf{t}_r , which is orthogonal to \mathbf{t}_1 and \mathbf{t}_2 . The difference from 4-hop WCNs is that every intermediate node needs to transmit \mathbf{t}_r to the previous node to acquire the corresponding radio channel coefficients for self-interference suppression. Once \mathbf{t}_r is back from the previous node, \mathbf{t}_r is deleted, and thus only the remaining \mathbf{t}_1 or \mathbf{t}_2 is forward or backward. For simplicity, the estimation error and residual noise are assumed to be Gaussian. The received training signal at \mathbb{T}_1 is

$$\mathbf{z}_1^{(N)} = \alpha_1 h_1 \mathbf{r}_1^{(N)} + \mathbf{n}_z^{(N)} = \prod_{i=1}^N \alpha_{2i-1} \mathbf{T} \mathbf{\Lambda}_z \mathbf{h}_z + \tilde{\mathbf{n}}_z, \quad (60)$$

where $\mathbf{\Lambda}_z = \text{diag}\left\{ \prod_{i=1}^{N-1} \alpha_{2i-1}, \prod_{i=1}^{N-1} \alpha_{2i} \right\}$, $\mathbf{h}_z = \text{diag}\left\{ \prod_{i=1}^N h_i^2, \prod_{i=1}^N h_i g_i \right\} = \text{diag}\{\varpi_1, \varpi_2\}$, $\tilde{\mathbf{n}}_{2N-1}^{(1)} = \sum_{i=1}^{N-1} \left[\left(\prod_{j=i}^{N-1} \alpha_{2j-1} h_{j+1} \right) \mathbf{n}_{2i-1}^{(1)} \right] + \sum_{i=1}^{N-1} \left[\left(\prod_{j=i}^{N-1} \alpha_{2j} g_{j+1} \right) \mathbf{n}_{2i}^{(1)} \right] + \mathbf{n}_{2N-1}^{(1)}$.

Proposition 4: When the number of communication nodes in $2N$ -hop WCNs approaches infinity, the MSE performance of ϖ_1 and ϖ_2 for the LMMSE scheme can be obtained respectively in certain situations as

$$\begin{aligned} \sigma_{\varpi_1}^2 &= \frac{\sigma_n^2}{(1-\omega)(1-\rho^2)Q_1}, \\ \sigma_{\varpi_2}^2 &= \frac{\sigma_n^2}{(1-\omega)(1-\rho^2)Q_2}. \end{aligned} \quad (61)$$

Similarly, the CRLB performance of ϖ_1 and ϖ_2 for the ML scheme can be obtained respectively in certain situations as

$$\begin{aligned} \text{CRLB}_{\varpi_1} &= \frac{\sigma_n^2}{(1-\omega)(1-\rho^2)Q_1}, \\ \text{CRLB}_{\varpi_2} &= \frac{\sigma_n^2}{(1-\omega)(1-\rho^2)Q_2}. \end{aligned} \quad (62)$$

Proof: See Appendix D. ■

VI. SIMULATION RESULTS

In this section, we numerically evaluate the presented channel estimation schemes along with the training design. The radio channels g_i and h_i of every hop are assumed to be circularly symmetric complex Gaussian random variables with zero means and unit variances. The transmission power of the desired nodes and intermediate nodes are assumed to be $P_1 = P_2 = P_{r1} = P_{r2} = P_{r3}$, and the variances of the noise generated at the desired nodes and intermediate nodes are assumed to be unity. The common signal-to-noise ratio (SNR) is defined as $P_1/\sigma_n^2 = P_1$. The length of the training sequences L is set as 8. The power of each symbol in the training sequences equals to P_1 , namely, the training power for Q_1 or Q_2 with the length of N is set as NP_1 . The correlation coefficients $|\rho| = 0$, $|\rho| = 0.5$, and $|\rho| = 0.9$ as three examples for comparisons are evaluated in simulations. Totally 10^5 Monte-Carlo runs are considered. Since the simulation results at \mathbb{T}_1 and \mathbb{T}_2 are symmetric and exchangeable, the following simulations are based on only the desired node \mathbb{T}_1 .

A. LMMSE Channel Estimation Schemes

The MSE performance for LMMSE estimation in 4-hop WCNs under different $|\rho|$'s is evaluated and compared in Fig. 4. LMMSE estimation achieves its best MSE performance when $|\rho|=0$ for all values of θ_1 and θ_2 , which is consistent with Lemma 1. The MSE gap increases when $|\rho|$ becomes large, which indicates that LMMSE estimation is significantly affected by the training structure and the optimal training design is vital in 4-hop MSNs. Moreover, the MSE discrepancy between θ_1 and θ_2 indicates that LMMSE estimation is sensitive to the statistical properties of the radio channel.

LMMSE estimation performance of 4-hop WCNs in terms of the average effective SNR (AESNR) is evaluated in Fig. 5, where the relationship between AESNR and SNR is shown. Orthogonal training is used in this simulation (i.e., $|\rho| = 0$). The dotted line is the theoretical bound of the AESNR obtained by assuming that perfect CSI is acquired at \mathbb{T}_1 . The solid line is the AESNR derived from the LMMSE method by taking the estimation errors into account. When the SNR is low, the LMMSE AESNR is far below the theoretical bound. As the SNR increases, the LMMSE AESNR approaches the theoretical bound, which demonstrates that LMMSE estimation is effective in 4-hop MSNs.

In Fig. 6, MSE performance is compared between the proposed LMMSE and the baseline point-to-point estimation scheme. In the baseline scheme, the training sequences are orthogonal to each other and the feedback estimated CSI is perfectly known at the desired nodes. It can be observed that the MSEs of θ_1 and θ_2 for LMMSE estimation are lower than that for point-to-point estimation in the region of high SNR, which demonstrates the effectiveness and performance gains of LMMSE estimation.

B. ML Channel Estimation Schemes

Similarly to LMMSE estimation, the MSE performance for θ_1 and θ_2 at different $|\rho|$'s when ML is utilized in 4-hop

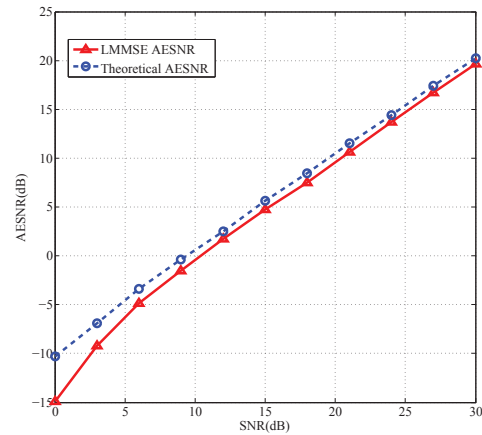


Fig. 4. Theoretical and LMMSE AESNR comparison with regards of SNR.

WCNs is shown in Fig. 7. It can be seen that ML achieves the best performance when $|\rho| = 0$, which is the same as LMMSE estimation. The MSE performance gaps increase with increasing SNR or when $|\rho|$ is large, which resembles the results for LMMSE estimation. The optimal training design can provide a significant accuracy performance gain for ML in 4-hop MSNs. In the low SNR region, the MSE of θ_2 is much larger than that of θ_1 because the estimation of θ_2 is indirectly obtained from the least-squares approach, which is based on the estimated $\hat{\theta}_1$. On the other hand, the MSE performance differences between θ_1 and θ_2 almost vanish in the high SNR region due to the increasing estimation precision of θ_1 .

The CRLBs of θ_1 and θ_2 versus SNR under different $|\rho|$'s in 4-hop WCNs are shown in Fig. 8. In the case of $|\rho| = 0$, the CRLBs of θ_1 and θ_2 achieve the best performance, which validates Lemma 3. Meanwhile, the optimal CRLB-based training structure coincides with optimal orthogonal training derived from ML and LMMSE estimation in the simulation as well as theoretical results.

C. Performance Evaluations for General $2N$ -Hop WCNs

When the 4-hop case is extended to the general $2N$ -hop case with $2N - 1$ intermediate nodes and two desired nodes, the MSE and CRLB performance versus N for LMMSE and ML estimation is compared in Fig. 9, where SNR is set at 0 dB, and $|\rho|$ is varied. The MSE performance of LMMSE estimation is lower than the CRLB performance of ML estimation when N is small, which indicates that LMMSE estimation often outperforms the unbiased ML estimation as it is derived to solely minimize the MSE. As N increases, the performance of the unbiased estimator approaches the LMMSE estimator and the MSE curves in Fig. 9 overlap with the CRLB curves under different $|\rho|$'s after a small number of relays, which corroborates with the analytical results in Section V. In addition, the MSE and CRLB performance under different $|\rho|$'s is shown in Fig. 9 as well. Similarly to results for 4-hop WCNs, the orthogonal training can achieve the best performance in $2N$ -hop MSNs, which indicates that the extension of the optimal orthogonal training design from 4-hop to $2N$ -hop WCNs is reasonable and effective.

In Fig. 10, MSE and CRLB performance is compared between Monte-Carlo simulation and theoretical analysis, where N is set at 8 and the value of $|\rho|$ is assumed to be 0. In the low SNR region, MSE and CRLB performance in the simulation are slightly worse than that of the theoretical analysis because the noise is approximated during the theoretical derivation. As SNR increases, the impact of noise diminishes, and performance of the simulated CRLB and MSE is close to that of the theoretical analysis.

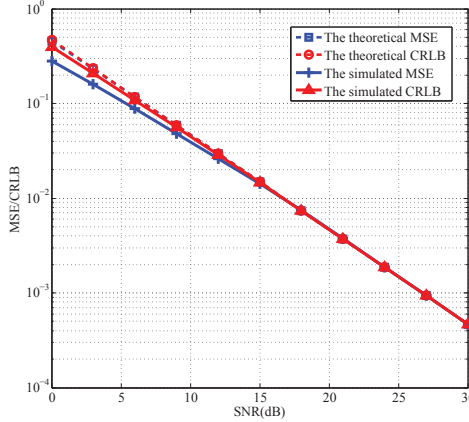


Fig. 5. MSE/CRLB comparisons between analysis and simulation.

VII. CONCLUSIONS

Motivated by the socially enabled user cooperation and multi-hop transmission in mobile sensor networks, the multi-hop wireless communication networks as the key communication technological component of MSNs have been studied in this paper. A bidirectional network coding multi-hop transmission strategy has been proposed, where the 4-hop WCNs has been studied first as the paradigm, followed by $2N$ -hop WCNs. To implement network coded MH-WCNs and improve transmission quality, radio channel estimation and the corresponding training design have been studied. Particularly, the LMMSE and ML radio channel estimation methods have been proposed in 4-hop WCNs firstly for the acquisition of composite channel coefficients at desired nodes. A closed-form MSE performance expression for the proposed LMMSE estimation scheme has been derived, and an optimal training scheme has been designed to minimize MSE. Due to the nonlinearity of ML radio channel estimation, design of the training sequences via minimizing CRLB has been exploited. Orthogonal training with the maximum allowable transmit power has been proved to be optimal for both CRLB and MSE performance criteria. According to the numerical and simulation results, both LMMSE and ML estimators have demonstrated effectiveness to improve the estimation accuracy in 4-hop WCNs. Meanwhile, the extension of the optimal orthogonal training design from 4-hop WCNs to $2N$ -hop WCNs has been shown to be reasonable and effective. This work improves the spectral efficiency and transmission quality of MH-WCNs, which can promote the successful use of MSNs in the future.

APPENDIX A PROOF OF LEMMA 1

The resulting MSE for the LMMSE scheme can be derived from [23] as

$$\sigma_{\theta}^2 = \text{tr}\{(\mathbf{R}_{\theta}^{-1} + \alpha_1^2 \tilde{\alpha}_3^2 \mathbf{\Lambda} \mathbf{T}^H \mathbf{R}_{\mathbf{n}}^{-1} \mathbf{T} \mathbf{\Lambda})^{-1}\}. \quad (63)$$

The MSE matrix in (63) can be expressed as

$$\begin{aligned} & (\mathbf{R}_{\theta}^{-1} + \alpha_1^2 \tilde{\alpha}_3^2 \mathbf{\Lambda} \mathbf{T}^H \mathbf{R}_{\mathbf{n}}^{-1} \mathbf{T} \mathbf{\Lambda})^{-1} \\ &= \frac{1}{\lambda} \begin{pmatrix} \frac{1}{\sigma_{\theta_2}^2} + \nu \alpha_2^2 [Q_2 + a_1(1 - \rho^2)Q_1Q_2] \\ -\nu \alpha_1 \alpha_2 [\rho \sqrt{Q_1Q_2} + a_3(1 - \rho^2)Q_1Q_2] \\ -\nu \alpha_1 \alpha_2 [\rho^* \sqrt{Q_1Q_2} + a_3^*(1 - \rho^2)Q_1Q_2] \frac{1}{\sigma_{\theta_1}^2} \\ +\nu \alpha_1^2 [Q_1 + a_2(1 - \rho^2)Q_1Q_2] \end{pmatrix}, \end{aligned} \quad (64)$$

where $a_1 = \frac{\alpha_1^2 \alpha_3^2}{\xi} \frac{\sigma_1^2 \sigma_3^2 \varepsilon}{(1 - |\rho|^2)Q_1}$, $a_2 = \frac{\alpha_1^2 \alpha_3^2}{\xi} \frac{\sigma_1^2 \sigma_3^2 \varepsilon}{(1 - |\rho|^2)Q_2}$, $a_3 = A_3$, $\nu = \frac{\alpha_1^2 \alpha_3^2}{\tau^* \xi \sigma_n^2}$ are defined for notational simplicity. The parameter λ can be written as

$$\begin{aligned} \lambda &= \frac{1}{\sigma_{\theta_1}^2 \sigma_{\theta_2}^2} + \nu^2 (1 - \rho^2) Q_1 Q_2 \tau^* \\ &+ \frac{1}{\sigma_{\theta_1}^2} \kappa \alpha_2^2 [Q_2 + a_1(1 - \rho^2)Q_1Q_2] \\ &+ \frac{1}{\sigma_{\theta_2}^2} \nu \alpha_1^2 [Q_1 + a_2(1 - \rho^2)Q_1Q_2]. \end{aligned} \quad (65)$$

To derive the expression in (65), the following substitutions are defined: $x = 1 - \rho^2$, $a = \frac{\alpha_1^2 \alpha_3^2 \sigma_1^2 \sigma_3^2 \varepsilon}{\xi}$, $b = \frac{\alpha_1^2 \alpha_3^2}{\sigma_n^2 \xi}$. The coefficients a_1, a_2, a_3 can be simplified as follows: $a_1 = \frac{a}{Q_1 x}$, $a_2 = \frac{a}{Q_2 x}$, $a_3 = -\frac{a \rho}{\sqrt{Q_1 Q_2} x}$, respectively. Substituting these simplified coefficients into τ^* , after re-organization, τ^* can be written as

$$\tau^* = 1 + \frac{2a}{x}(1 - \rho^2) + a^2 \frac{(1 - \rho^2)^2}{x^2} = (1 + a)^2. \quad (66)$$

Then, ν can be rewritten as $\nu = b/(1 + a)^2$. Therefore, after some algebra, the MSE performance σ_{θ}^2 can be written as

$$\sigma_{\theta}^2 = \frac{1}{\lambda \sigma_{\theta_1}^2 \sigma_{\theta_2}^2} \left[\sigma_{\theta_1}^2 + \sigma_{\theta_2}^2 + \frac{b}{1 + a} (\alpha_2^2 Q_2 + \alpha_1^2 Q_1) \sigma_{\theta_1}^2 \sigma_{\theta_2}^2 \right]. \quad (67)$$

Further, λ can be simplified as

$$\begin{aligned} \lambda &= \frac{1}{\sigma_{\theta_1}^2 \sigma_{\theta_2}^2} + \frac{b}{(1 + a) \sigma_{\theta_1}^2} \alpha_2^2 Q_2 \\ &+ \frac{b}{(1 + a) \sigma_{\theta_2}^2} \alpha_1^2 Q_1 + \frac{b^2}{(1 + a)^2} x \alpha_1^2 \alpha_2^2 Q_1 Q_2. \end{aligned} \quad (68)$$

Since σ_{θ}^2 is a positive coefficient independent of the correlation coefficient ρ , it is monotonically decreasing with λ . Meanwhile, λ monotonically increases with x and decreases with ρ , and the MSE σ_{θ}^2 can be proven to be proportional to the correlation coefficient ρ and achieves its minimum when $\rho = 0$, which means the best training should be orthogonal.

Taking the optimal value $|\rho| = 0$, the MSE σ_θ^2 can be rewritten as

$$\sigma_\theta^2 = \frac{\sigma_{\theta_1}^2 + \sigma_{\theta_2}^2 + \frac{b}{1+a}(\alpha_2^2 Q_2 + \alpha_1^2 Q_1)\sigma_{\theta_1}^2 \sigma_{\theta_2}^2}{(1 + \frac{b}{1+a}\alpha_1^2 \sigma_{\theta_1}^2 Q_1)(1 + \frac{b}{1+a}\alpha_2^2 \sigma_{\theta_2}^2 Q_2)}. \quad (69)$$

The maximum training power assigned to \mathbf{t}_i is assumed to be Q_i^{max} , which is typically equal to LP_i (P_i is the transmission power at \mathbb{T}_i). Thus, the optimal power can be allocated as $\|\mathbf{t}_i\|^2 \in [0, Q_i^{max}]$ by minimizing σ_θ^2 . The derivatives of σ_θ^2 with respect to Q_1 and Q_2 are given by

$$\frac{\partial \sigma_\theta^2}{\partial Q_1} = -\frac{1}{B_0} \left[\frac{b}{1+a} \alpha_1^2 \sigma_{\theta_1}^4 + \left(\frac{b}{1+a} \right)^2 \alpha_1^2 \alpha_2^2 \sigma_{\theta_1}^4 \sigma_{\theta_1}^2 Q_2 \right] < 0, \quad (70)$$

$$\frac{\partial \sigma_\theta^2}{\partial Q_2} = -\frac{1}{B_0} \left[\frac{b}{1+a} \alpha_2^2 \sigma_{\theta_2}^4 + \left(\frac{b}{1+a} \right)^2 \alpha_1^2 \alpha_2^2 \sigma_{\theta_1}^2 \sigma_{\theta_1}^4 Q_1 \right] < 0, \quad (71)$$

respectively. Obviously, σ_θ^2 monotonically decreases with the training power Q_i . Therefore, the optimal power allocation requires that both desired nodes should transmit the training sequences with their maximum allowable transmit power.

APPENDIX B PROOF OF PROPOSITION 2

Defining $\boldsymbol{\theta}_r = [\Re\{\boldsymbol{\theta}\}^T, \Im\{\boldsymbol{\theta}\}^T]^T$, the complex Fisher Information Matrix (FIM) can be expressed as

$$\mathbf{F}_{uv} = \mathcal{E} \left\{ \left(\frac{\partial \log p(\mathbf{z}_3|\boldsymbol{\theta})}{u^*} \right) \left(\frac{\partial \log p(\mathbf{z}_3|\boldsymbol{\theta})}{v^*} \right)^H \right\}. \quad (72)$$

Following [25], the CRLB of $\boldsymbol{\theta}_r$ is

$$\text{CRLB} = \mathbf{F}_{\boldsymbol{\theta}_r, \boldsymbol{\theta}_r}^{-1}, \quad (73)$$

where $\mathbf{F}_{\boldsymbol{\theta}_r, \boldsymbol{\theta}_r} = \mathbf{M} \begin{bmatrix} \mathbf{F}_{\boldsymbol{\theta}\boldsymbol{\theta}} & \mathbf{F}_{\boldsymbol{\theta}\boldsymbol{\theta}^*} \\ \mathbf{F}_{\boldsymbol{\theta}^*\boldsymbol{\theta}} & \mathbf{F}_{\boldsymbol{\theta}^*\boldsymbol{\theta}^*} \end{bmatrix} \mathbf{M}^H$, $\mathbf{M} = \begin{bmatrix} \mathbf{I} & \mathbf{I} \\ -j\mathbf{I} & j\mathbf{I} \end{bmatrix}$,

The derivatives of the log-likelihood function with respect to θ_1 and θ_2 can be derived as

$$\frac{\partial \log p(\mathbf{z}_3|\boldsymbol{\theta})}{\theta_1^*} = \alpha_1 \alpha_2 \tilde{\alpha}_3 (\alpha_1 \tilde{\alpha}_3 h_1 h_2 \tilde{\mathbf{n}}_r^{(1)} + \bar{\mathbf{n}})^H \mathbf{R}_{\bar{\mathbf{n}}}^{-1} \mathbf{t}_2. \quad (74)$$

Substituting the derivatives (74) into the FIM in (72), $\mathbf{F}_{\boldsymbol{\theta}\boldsymbol{\theta}}$ and $\mathbf{F}_{\boldsymbol{\theta}\boldsymbol{\theta}^*}$ can be written in an abbreviated form:

$$\mathbf{F}_{\boldsymbol{\theta}\boldsymbol{\theta}} = \begin{bmatrix} D_1 & D_2 \\ D_2^* & D_3 \end{bmatrix}, \quad \mathbf{F}_{\boldsymbol{\theta}\boldsymbol{\theta}^*} = \begin{bmatrix} D_4 & 0 \\ 0 & 0 \end{bmatrix}, \quad (75)$$

respectively. Then CRLB_{θ_1} and CRLB_{θ_2} can be derived from the CRLB by

$$\text{CRLB}_{\theta_1} = [\text{CRLB}]_{11} + [\text{CRLB}]_{33}, \quad (76)$$

$$\text{CRLB}_{\theta_2} = [\text{CRLB}]_{22} + [\text{CRLB}]_{44}. \quad (77)$$

Consequently, the results of (55) and (56) are proven.

APPENDIX C PROOF OF LEMMA 3

As D_2 is only related to $|\rho|$, derivatives of CRLB_{θ_1} and CRLB_{θ_2} can be taken with respect to $|D_2|^2$ as

$$\frac{\partial \text{CRLB}_{\theta_1}}{\partial |D_2|^2} = \frac{D_3 [(|D_2|^2 - D_1 D_2)^2 + |D_4|^2 D_3^2]}{[(|D_2|^2 - D_1 D_3)^2 - |D_4|^2 D_3^2]^2} > 0, \quad (78)$$

$$\begin{aligned} \frac{\partial \text{CRLB}_{\theta_2}}{\partial |D_2|^2} &= \frac{D_1 |D_2|^4 - 2D_3 (D_1^2 - |D_4|^2) |D_2|^2}{[(|D_2|^2 - D_1 D_3)^2 - |D_4|^2 D_3^2]^2} \\ &+ \frac{D_1^2 D_3^2 (D_1^2 - |D_4|^2)}{[(|D_2|^2 - D_1 D_3)^2 - |D_4|^2 D_3^2]^2} > 0. \end{aligned} \quad (79)$$

Obviously, CRLB_{θ_1} is an increasing function of $|\rho|^2$ due to the fact that (78) is positive. When $|\rho| = 0$, CRLB_{θ_1} reaches its minimum value. While for CRLB_{θ_2} , its numerator can be re-expressed as

$$D_1 \left[|D_2|^2 - \frac{D_3}{D_1} (D_1^2 - |D_4|^2) \right]^2 + \frac{D_3^2}{D_1} (D_1^2 - |D_4|^2) |D_4|^2. \quad (80)$$

When $|D_4|^2 < D_1^2$, (79) is positive. Therefore, both CRLB_{θ_1} and CRLB_{θ_2} are increasing functions of $|\rho|^2$, which achieve their minimum values at $|\rho| = 0$. Namely, the optimal \mathbf{t}_1 and \mathbf{t}_2 should be orthogonal. When $|\rho| = 0$, the corresponding CRLBs can be expressed as

$$\text{CRLB}_{\theta_1} = \frac{D_1}{D_1^2 - |D_4|^2}, \quad (81)$$

$$\text{CRLB}_{\theta_2} = \frac{1}{D_3}. \quad (82)$$

It is supposed that the maximum power assigned to \mathbf{t}_i is Q_i^{max} (typically LP_i). By minimizing CRLBs, the optimal training power assigned for each \mathbf{t}_i can be achieved. The optimal training power for CRLB_{θ_1} is LP_{r2} , which means the desired node \mathbb{T}_2 needs to transmit with its maximum allowable transmit power. For CRLB_{θ_2} , the corresponding optimization for Q_1 is

$$Q_1 = \arg \min_{Q_1} \frac{Q_1 + c}{Q_1^2 + 2cQ_1}, \quad (83)$$

where $c = \frac{a_0 \sigma_n^2 (r-2)^2}{4(1+a)}$. Since the objective function is a decreasing function of Q_1 , the optimal training power for \mathbb{T}_1 is achieved with the maximum allowable transmit power Q_1^{max} .

APPENDIX D PROOF OF PROPOSITION 4

Firstly, the corresponding covariance matrix of the equivalent noise is

$$\begin{aligned} \mathbf{R}_{\bar{\mathbf{n}}_z} &= \left\{ 1 + \sum_{i=1}^{N-1} \left(\prod_{j=i}^{N-1} \alpha_{2j-1}^2 \sigma_{2j-1}^2 \right) \right. \\ &+ \sum_{i=1}^{N-1} \left[\prod_{k=1}^N \alpha_{2k-1}^2 \sigma_{2k-1}^2 \left(\prod_{j=i}^{N-1} \alpha_{2j}^2 \sigma_{2j}^2 \right) + \alpha_{2N-1}^2 \sigma_1^2 \right. \\ &\left. \left. \prod_{k=1}^{i-1} \alpha_{2k-3}^2 \sigma_{2k-1}^2 \left(2^{N-i} \prod_{j=i}^{N-1} \alpha_{2j-1}^4 \sigma_{2j+1}^4 \right) \right] \right\} \sigma_n^2 \mathbf{I}. \end{aligned} \quad (84)$$

As the number of nodes N increases, $\mathbf{R}_{\bar{n}_z}$ reaches the upper bound under certain circumstances. The transmit power is assumed to be P , and the channel gains are assumed to have the same variance σ . On denoting $\alpha_i^2 \sigma_i^2$ by ω , and substituting the simplified expression into $\mathbf{R}_{\bar{n}_z}$, (84) can be rewritten as

$$\mathbf{R}_{\bar{n}_z} = \left[\frac{1 - \omega^N + \omega^{N+1} - \omega^{2N}}{1 - \omega} + \frac{2\omega^{N+1} [1 - (2\omega)^{N-1}]}{1 - 2\omega} \right] \sigma_n^2 \mathbf{I}. \quad (85)$$

When N approaches to infinity, the upper bound of $\mathbf{R}_{\bar{n}_z}$ can be written as

$$\lim_{n \rightarrow \infty} \mathbf{R}_{\bar{n}_z} = \frac{1}{1 - \omega} \sigma_n^2 \mathbf{I}. \quad (86)$$

Similarly to the 4-hop WCNs, the performance of LMMSE for the $2N$ -hop case can be derived conditionally. The MSE of \mathbf{h}_z can be expressed as

$$\begin{aligned} \sigma_{\mathbf{h}_z}^2 &= \text{tr} \left\{ \left(\mathbf{R}_{\mathbf{h}_z}^{-1} + \prod_{i=1}^N \alpha_{2i-1} \mathbf{\Lambda}_z \mathbf{T}^H \mathbf{R}_{\bar{n}_z}^{-1} \mathbf{T} \mathbf{\Lambda}_z \right)^{-1} \right\} \\ &= \text{tr} \left\{ \left(\text{diag} \{ 2^N \sigma^{4N}, \sigma^{4N} \}^{-1} + \frac{\kappa^{2N-1}}{\eta \sigma_n^2} \mathbf{T}^H \mathbf{T} \right)^{-1} \right\}, \end{aligned} \quad (87)$$

where κ represents α_i^2 . If $\kappa < 1$, the parameter $\frac{\kappa^{2n-1}}{\eta \sigma_n^2}$ is equal to zero, which indicates that the MSE can be expressed as $\sigma_{\mathbf{h}_z}^2 = (1 + 2^n) \sigma^{4n}$. If $\sigma^2 > \sqrt{2}/2$, there is no upper bound for the MSE. When $\sigma^2 = \sqrt{2}/2$, the MSE is simply equal to one. Obviously, the MSE approaches zero if the variance satisfies $\sigma^2 < \sqrt{2}/2$. If the amplification factor is equal to one, $\frac{\kappa^{2n-1}}{\eta \sigma_n^2} = \frac{1-\omega}{\sigma_n^2}$ remains constant. When $\sigma^2 > 1$, the MSE performance of ϖ_1 and ϖ_2 can be derived as $\sigma_{\varpi_1}^2 = \frac{\sigma^2}{(1-\omega)(1-\rho^2)Q_1}$ and $\sigma_{\varpi_2}^2 = \frac{\sigma^2}{(1-\omega)(1-\rho^2)Q_2}$, respectively.

In the case of the amplification factor $\kappa > 1$, the parameter $\frac{\kappa^{2n-1}}{\eta \sigma_n^2}$ approaches infinity and the MSE cannot be obtained directly. Similarly, we can derive the CRLBs for $2N$ -hop WCNs in the same way we did for 4-hop WCNs. In brief, only the case when the amplification $\alpha_i = 1$ is considered; the coefficients D_i in the CRLB can be transformed as $D_1 = \frac{(1-\omega)Q_1}{\sigma_n^2}$, $D_2 = \frac{\rho(1-\omega)\sqrt{Q_1 Q_2}}{\sigma_n^2}$, $D_3 = \frac{(1-\omega)Q_2}{\sigma_n^2}$, and $D_4 = 0$.

The CRLB for ϖ_1 and ϖ_2 in $2N$ -hop WCNs can be derived respectively as $\text{CRLB}_{\varpi_1} = \frac{\sigma_n^2}{(1-\omega)(1-\rho^2)Q_1}$ and $\text{CRLB}_{\varpi_2} = \frac{\sigma_n^2}{(1-\omega)(1-\rho^2)Q_2}$. It is noted that CRLBs are almost the same as the MSE. Moreover, the same conclusions in 4-hop WCNs can be extended to $2N$ -hop WCNs in special cases when the optimal training is orthogonal and the maximum allowable transmit power is used.

REFERENCES

- [1] N. Kayastha, D. Niyato, P. Wang, and E. Hossain, "Applications, architectures, and protocol design issues for mobile social networks: A survey," *Proceedings of IEEE*, vol. 99, no. 12, pp. 2130–2158, Dec. 2011.
- [2] A. Weaver, and B. Morrison, "Social networking," *IEEE Computer*, vol. 41, no. 2, pp. 97–100, Feb. 2008.
- [3] E. Stai, V. Karyotis, and S. Papavassiliou, "Topology enhancements in wireless multi-hop networks: A top-down approach," *IEEE Trans. Parallel and Distributed Systems*, vol. 23, no. 7, pp. 1344–1357, July 2012.
- [4] K. C. Chen, M. Chiang, and H. V. Poor, "From technological networks to social networks," *IEEE J. Sel. Areas Commun.*, vol. 31, no. 9, pp. 548C–572, Sep. 2013.
- [5] A. Eryilmaz and R. Srikant, "Joint congestion control, routing and MAC for stability and fairness in wireless networks," *IEEE J. Sel. Areas Commun.*, vol. 24, no. 8, pp. 1514–1524, Aug. 2006.
- [6] K. C. Chen, H. V. Poor, and R. Prasad, "Mobile social networks [Guest Editorial]," *IEEE Wireless Commun.*, vol. 21, no. 1, pp. 8–9, Feb. 2014.
- [7] X. Liang, K. Zhang, X. Shen, and X. Lin, "Security and privacy in mobile social networks: challenges and solutions," *IEEE Wireless Commun.*, vol. 21, no. 1, pp. 33–41, Feb. 2014.
- [8] J. Munoz, J. Garzon, P. Ameigeiras, J. Ortíz, and J. Soler, "Characteristics of mobile youtube traffic," *IEEE Wireless Commun.*, vol. 21, no. 1, pp. 18–25, Feb. 2014.
- [9] E. Stai, V. Karyotis, and S. Papavassiliou, "Exploiting socio-physical network interactions via a utility-based framework for resource management in mobile social networks," *IEEE Wireless Commun.*, vol. 21, no. 1, pp. 10–17, Feb. 2014.
- [10] A. Sendonaris, E. Erkip, and B. Aazhang, "User cooperation diversity: Part I. System description," *IEEE Trans. Commun.*, vol. 51, no. 11, pp. 1927–1938, Nov. 2003.
- [11] A. Nosratinia, T. Hunter, and A. Hedayat, "Cooperative communication in wireless networks," *IEEE Commun. Magazine*, vol. 42, no. 10, pp. 74–80, Oct. 2004.
- [12] R. Ahlswede, N. Cai, S. Li, and R. Yeung, "Network information flow," *IEEE Trans. Inform. Theory*, vol. 46, no. 4, pp. 1204–1216, July 2000.
- [13] S. Sengupta, S. Rayanchu, and S. Banerjee, "Network coding-aware routing in wireless networks," *IEEE/ACM Trans. Networking*, Vol. 18, No. 4, pp. 1158–1170, Aug. 2010.
- [14] R. Prior, D. Lucani, Y. Phulpin, M. Nistor, and J. Barros, "Network coding protocols for smart grid communications," *IEEE Trans. Smart Grid*, 2014.
- [15] N. S. Riberio Júnior, et al., "CodeDrip: Data dissemination protocol with network coding for wireless sensor networks," *Wireless Sensor Networks*, Springer International Publishing, pp: 34–49, 2014.
- [16] P. Pahlavani, D. ELucani, M. Pedersen, and F. Fitzek, "PlayNCool: opportunistic network coding for local Optimization of routing in wireless mesh networks," in *Proc. IEEE GLOBECOM Workshops*, Alantata, GA, Dec. 2013, pp. 812–817.
- [17] F. Fitzek, J. Heide, M. V. Pedersen, and M. Katz, "Implementation of network coding for social mobile clouds," *IEEE Signal Processing Magazine* vol. 30, no. 1, Jan. 2013.
- [18] S. Li, R. Yeung, and N. Cai, "Linear network coding," *IEEE Trans. Inform. Theory*, vol. 49, no. 2, pp. 371–381, Feb. 2003.
- [19] F. Gao, R. Zhang, and Y. Liang, "Optimal channel estimation and training desing for two-way relay networks," *IEEE Trans. Commun.*, vol. 57, no. 10, pp. 3024–3033, Oct. 2009.
- [20] B. Jiang, F. Gao, X. Gao, and A. Nallanathan, "Channel estimation and training desing for two-way relay networks with power allocation," *IEEE Trans. Wireless Commun.*, vol. 9, no. 6, pp. 2022–2032, Jun. 2010.
- [21] X. Xie, M. Peng, B. Zhao, W. Wang, and Y. Hua, "Maximum a posteriori based channel estimation strategy on two-way relaying channels," *IEEE Trans. Wireless Communi.*, vol. 13, no. 1, pp. 450–463, Jan. 2014.
- [22] F. Tabataba, P. Sadeghi, C. Hucher, and M. Pakravan, "Impact of channel estimation errors and power allocation on analog network coding and routing in two-way relaying," *IEEE Trans. Vehicular Tech.*, vol. 61, no. 7, pp. 3223–3239, Sep. 2012.
- [23] S. Kay, *Fundamentals of Statistical Signal Processing: Estimation Theory*, Englewood Cliffs NJ: Prentice Hall, 1987.
- [24] M. Sichitui and C. Veerarittiphan, "Simple, accurate time synchronization for wireless sensor networks," in *Proc. IEEE Wireless Communications and Networking Conference (WCNC)*, New Orleans, LA, Mar. 2003, pp. 1266–1273.
- [25] E. de Carvalho, J. Cioffi, and D. Slock, "Cramér-rao bounds for blind multichannel estimation," in *Proc. IEEE GLOBECOM*, San Francisco, CA, Nov. 2000, pp. 1036–1040.

PLACE
PHOTO
HERE

Mugen Peng (M'05–SM'11) received the Ph.D. degree in communication and information system from the Beijing University of Posts & Telecommunications (BUPT), China, in 2005. After the Ph.D. graduation, he joined BUPT, and became a full professor with the School of Information and Communication Engineering, BUPT, in October 2012. During 2014, he is also an academic visiting fellow with Princeton University, Princeton, NJ, USA. He is leading a research group focusing on wireless transmission and networking technologies in the Key Laboratory of Universal Wireless Communications (Ministry of Education) at BUPT. His main research areas include wireless communication theory, radio signal processing and convex optimizations, with particular interests in cooperative communication, radio network coding, self-organizing network, heterogeneous network, and cloud computing. He has authored/coauthored more than 40 refereed IEEE journal papers and over 200 conference proceeding papers.

Dr. Peng is currently on the Editorial/Associate Editorial Board of *IEEE Communications Magazine*, *IEEE Access*, *International Journal of Antennas and Propagation (IJAP)*, *China Communication*, and *International Journal of Communications System (IJCS)*. He has been the guest leading editor for special issues of *IEEE Wireless Communications*, *IJAP* and the *International Journal of Distributed Sensor Networks (IJDSN)*. Dr. Peng was honored with the 2014 IEEE ComSoc AP Outstanding Young Researcher Award, and the Best Paper Award in GameNets 2014, CIT 2014, ICCTA 2011, IC-BNMT 2010, and IET CCWMC 2009. He was awarded the First Grade Award of Technological Invention by the Ministry of Education of China for his excellent research work on hierarchical cooperative communication theory and technologies, and the Second Grade Award of Scientific & Technical Progress from the China Institute of Communications for his excellent research work on the co-existence of multi-radio access networks and 3G spectrum management in China.

PLACE
PHOTO
HERE

H. Vincent Poor (S'72, M'77, SM'82, F'87) received the Ph.D. degree in EECS from Princeton University in 1977. From 1977 until 1990, he was on the faculty of the University of Illinois at Urbana-Champaign. Since 1990 he has been on the faculty at Princeton, where he is the Michael Henry Strater University Professor of Electrical Engineering and Dean of the School of Engineering and Applied Science. Dr. Poor's research interests are in the areas of stochastic analysis, statistical signal processing, and information theory, and their applications in wireless networks and related fields such as social networks and smart grid. Among his publications in these areas are the recent books *Principles of Cognitive Radio* (Cambridge University Press, 2013) and *Mechanisms and Games for Dynamic Spectrum Allocation* (Cambridge University Press, 2014).

Dr. Poor is a member of the National Academy of Engineering and the National Academy of Sciences, and a foreign member of Academia Europaea and the Royal Society. He is also a fellow of the American Academy of Arts and Sciences, the Royal Academy of Engineering (U.K.), and the Royal Society of Edinburgh. He received the Marconi and Armstrong Awards of the IEEE Communications Society in 2007 and 2009, respectively. Recent recognition of his work includes the 2014 URSI Booker Gold Medal, and honorary doctorates from several universities in Europe and Asia, including an honorary D.Sc. from Aalto University in 2014.

PLACE
PHOTO
HERE

Qiang Hu received the B.S. degree in applied physics from the Beijing University of Posts & Communications (BUPT), China, in 2013. He is currently pursuing the Master degree at BUPT. His research interests include cooperative communications, such as cloud radio access networks (C-RANs), and statistical signal processing in large-scale networks.

PLACE
PHOTO
HERE

Xinqian Xie received the B.S. degree in telecommunication engineering from the Beijing University of Posts and Communications (BUPT), China, in 2010. He is currently pursuing the Ph.D. degree at BUPT. His research interests include cooperative communications, estimation and detection theory.

PLACE
PHOTO
HERE

Zhongyuan Zhao is currently a lecturer with the Key Laboratory of Universal Wireless Communication (Ministry of Education) at the Beijing University of Posts & Telecommunications (BUPT), China. He received his Ph.D. degree in communication and information systems and B.S. degree in applied mathematics from BUPT in 2009 and 2014, respectively. His research interests include network coding, MIMO, relay transmissions, and large-scale cooperation in future communication networks.